JLB

Article

Role of interleukin-18 in intrahepatic inflammatory cell recruitment in acute liver injury

Kiminori Kimura,[*,†,1] Satoshi Sekiguchi,[†] Seishu Hayashi,[*] Yukiko Hayashi,[‡] Tsunekazu Hishima,[‡] Masahito Nagaki,[§] and Michinori Kohara[†]*

Divisions of *Hepatology and [‡]Pathology, Tokyo Metropolitan Cancer and Infectious Diseases Center, Komagome Hospital, Tokyo, Japan; [†]Department of Microbiology and Cell Biology, Tokyo Metropolitan Institute of Medical Science, Tokyo, Japan; and [§]Department of Gastroenterology, Gifu University Graduate School of Medicine, Gifu, Japan

RECEIVED JULY 20, 2010; REVISED OCTOBER 12, 2010; ACCEPTED NOVEMBER 9, 2010. DOI: 10.1189/jlb.0710412

ABSTRACT

Although the innate immune system has been demonstrated to play important roles as the first line of defense against various infections, little is known about the interactions between intrahepatic inflammatory cells and the cytokine network in the liver. Here, we examined the role of IL-18 in IHL recruitment in acute liver injury. C57BL/6 mice were injected with an αCD40 mAb, and their serum IL-18 levels were observed to increase, with subsequent recruitment of IHLs into the liver. NKT cells were involved in this liver injury, as the serum ALT levels were reduced in NKT KO mice through the suppression of macrophage and monocyte migration and cytokine production. In contrast, depletion of neutrophils exacerbated the liver injury associated with high levels of TNF-α and IL-18 and increased numbers of macrophages and monocytes. Treatment with a neutralizing antibody against IL-18 reduced the serum ALT levels and inflammatory cell accumulation in the liver. Finally, additional administration of rIL-18 with αCD40 injection caused severe liver injury with increased IFN-γ production by NK cells. In conclusion, these findings demonstrate that IL-18 modulates liver inflammation by the recruitment of inflammatory cells, including NKT cells, macrophages, monocytes, and neutrophils. *J. Leukoc. Biol.* 89: 433–442; 2011.

Introduction

Macrophages of the innate immune system are the first line of defense against many pathogens and play a crucial role in the elimination of bacterial infections [1]. The resident liver macrophages, Kupffer cells, are well known to be phagocytic macrophages and account for 80% of the total population of fixed tissue macrophages in the body [2]. These cells are derived from blood monocytes and found mainly in the hepatic sinusoid [3]. They are continuously exposed to various pathogenic components, such as the gram-negative bacteria cell wall constituent LPS, and have the ability to protect their host immediately from the associated bacteria. Activated macrophages can also secrete inflammatory cytokines, such as TNF-α, IL-12, IL-18 [4, 5], and chemokines [6], in response to certain stimuli. These mediators produced by macrophages and the capacity for phagocytosis are essential for protection against microorganisms [7].

In contrast, NKT cells express an invariant TCR chain (V14-J281 in mice) and recognize glycolipid antigens, such as α-galactosylceramide, in association with the MHC class I-like molecule CD1d [8]. APCs, including DCs and macrophages, present antigens to NKT cells, a process that is dependent on CD40 ligation and results in the rapid release of large amounts of Th1 and Th2 cytokines and chemokines. Activated NKT cells can also provide maturation signals for other inflammatory cells, especially DCs, NK cells, and macrophages, thereby involving innate and acquired immunity [9, 10].

IL-18 is a member of the IL-1 family that is produced as a biologically inactive precursor and secreted after activation by cleavage with caspase-1 or other caspases [11]. Originally, IL-18 was identified as an IFN-γ-inducing factor that can act on Th1 cells, nonpolarized T cells, NK cells, B cells, and DCs to produce IFN-γ in the presence of IL-12 [12]. Besides its potent induction of IFN-γ, IL-18 activates NK and T cells, which play central roles in viral clearance [13].

We have already demonstrated that αCD40 mAb injection induces biphasic liver injury by way of inflammatory cytokine and chemokine production [14]. Furthermore, this liver injury requires NK cells and macrophages in the early-phase events, and B cells also contribute to the late-phase liver inflammation [15]. During analyses of this liver injury model, we found that

Abbreviations: αCD40=anti-CD40, ALT=alanine aminotransferase, IHL=intrahepatic leukocyte, KO=knockout (deficient), NLR=NOD-like receptor

The online version of this paper, found at www.jleukbio.org, includes supplemental information.

1. Correspondence: Division of Hepatology, Tokyo Metropolitan Cancer and Infectious Diseases Center, Komagome Hospital, 18-22-3 Honkomagome, Bunkyo-ku, Tokyo 113-8677, Japan. E-mail: kkimura@cick.jp

serum IL-18 was increased dramatically at the late phase. In the present study, we investigated the involvement of IL-18 in the liver injury and focused on the interactions among IL-18 and NKT cells, neutrophils, macrophages, and monocytes, which play important roles in various diseases. The results obtained provide new insights into the inflammatory network among macrophages, neutrophils, and NKT cells during liver injury.

MATERIALS AND METHODS

Mice

Vα14 NKT KO mice were generated as described [7], and C57BL/6 mice were purchased from Japan SLC (Shizuoka, Japan). All animals were housed in pathogen-free rooms under strict barrier conditions and received humane care according to the guidelines of the Animal Care Committees of Gifu University School of Medicine (Gifu, Japan) and Tokyo Metropolitan Institute of Medical Science (Tokyo, Japan).

Antibodies

Mice were injected i.v. with 100 μg αCD40 [16] or 100 μg purified rat IgG2a as a control (BD PharMingen, San Diego, CA, USA). In addition, some mice were injected i.p. (200 μg/mouse) at Days −1, +1, and +3 with a rat mAb against mouse Gr-1 (clone RB6-8C5) and control rat IgG2b (both from eBioscience, San Diego, CA, USA). At Days −1, +1, and +3, other mice were injected i.p. with a rat anti-mouse IL-18 mAb (50 μg/mouse) and rat IgG (both from MBL, Nagoya, Japan).

Cell isolation

To isolate IHLs, single-cell suspensions were prepared from liver perfused with PBS via the inferior vena cava and digested in 10 mL RPMI 1640 (Life Technologies, Gaithersburg, MD, USA) containing 0.02% (wt/vol) collagenase IV (Sigma-Aldrich, St. Louis, MO, USA) and 0.002% (wt/vol) DNase I (Sigma-Aldrich) for 40 min at 37°C. Cells were overlaid on Lympholyte M (Cedarlane, Westbury, NY, USA) in PBS. Bone marrow cells were collected from the femurs and tibias of mice. To isolate PBMCs, peripheral blood (0.4 mL) was obtained by cardiac puncture under ether anesthesia. After density separation, cell counts and immunofluorescence analyses were performed.

Tissue RNA analyses

Frozen livers were mechanically pulverized under liquid nitrogen, and total RNAs were isolated for RPAs as described previously [15]. All reagents for the RPAs were purchased from BD PharMingen.

ELISA

The serum IL-18, TNF-α, and IFN-γ concentrations were assayed using specific ELISA kits (IL-18, MBL; TNF-α and IFN-γ, Genzyme Techne Corp., Minneapolis, MN, USA), according to each corresponding manufacturer's protocols.

Immunohistochemistry

The samples were embedded in OCT compound (Tissue Tek, Miles, Elkhart, IN, USA) and frozen in liquid nitrogen. Sections were cut at 4 μm thickness using a cryostat and fixed with cold acetone for 10 min. The fixed sections were treated with rat anti-mouse F4/80, Ly-6C, and Gr-1 mAb (10 μg/mL), followed by a streptavidin-biotin-HRP complex (Dako, Glostrup, Denmark). The positive reactions were visualized with 0.035% H_2O_2 and 0.03% 3,3′-diaminobenzidine (Wako, Tokyo, Japan) in 50 mM Tris-HCl (pH 7.6) for 2–3 min. After 4% formaldehyde fixation, the stained sections were counterstained with hematoxylin and subjected to microscopic observation.

Flow cytometry

The cells were surface-stained with fluorochrome-conjugated mAb for 20 min on ice. The following antibodies were used: anti-CD3, anti-NK1.1, anti-CD11b, and anti-CD11c (all from eBioscience). The F4/80 and Ly-6C mAb (BMA Biomedicals, Geneva, Switzerland) were also used. In addition, the cells were surface-stained with FITC-conjugated anti-CD3, FITC-conjugated anti-CD11b, and allophycocyanin-conjugated anti-NK1.1 mAb, together with anti-IFN-γ-PE and anti-TNF-α-PE mAb (all from BD PharMingen) for intracellular cytokine detection. Samples were acquired using a FACSCalibur flow cytometer, and data were analyzed using the CellQuest software (BD Immunocytometry Systems, San Jose, CA, USA) and FlowJo software (Tree Star, San Carlos, CA, USA).

BrdU incorporation

For in vivo BrdU labeling, mice received a 100-μL i.p. injection of a 10-mg/mL solution of BrdU in PBS at 2 h before sacrifice. Single-cell suspensions of IHLs were prepared at 24 h after αCD40 injection and surface-stained with PE-CD11b. Following the surface staining, the cells were fixed, stained for intracellular BrdU using a FITC-BrdU flow kit (BD PharMingen), and analyzed by flow cytometry.

Data analysis

All data are expressed as the mean + SD. Values of $P < 0.05$ were considered statistically significant.

RESULTS

A single injection of αCD40 increases serum IL-18

We found that the serum ALT activity began to elevate on Day 1 and was clearly increased on Day 5 after αCD40 injection. We confirmed further that inflammatory cytokine and chemokine mRNA expressions were increased at Days 1 and 5 in C57BL/6 mice (Supplemental Fig. 1A). We measured the serum IL-18 level and found that it began to increase at Day 3 and was remarkably increased until Day 5 after the injection. To determine the infiltration of inflammatory cells in the same livers, we counted the absolute number of IHLs and calculated the number of cells in each IHL subset. As shown in **Fig. 1B**, Gr-1^{++}/CD$11b^{+}$ cells (mostly neutrophils) were increased until Day 1 and then decreased at Days 3 and 5. On the other hand, Gr-1^{+}/CD$11b^{+}$ cells (mostly macrophages and monocytes) were increased and reached a peak at Day 3 and then decreased until Day 5. Furthermore, to evaluate the numbers of macrophages and their precursors in the liver, the cells were stained with the CD11b, F4/80, and Ly-6C mAb, which recognize antigens on macrophages and their precursors at different stages of differentiation [17]. The numbers of Ly-$6C^{++}$/CD$11b^{+}$ cells (mostly monocytes) and F4/80^{+}/CD$11b^{+}$ cells (tissue macrophages) began to increase by Day 1, reached a peak at Day 3, and then decreased until Day 5. In immunohistochemical analyses, Gr-1^{+} cells were increased at Day 1 in the liver parenchyma, whereas Ly-$6C^{+}$ and F4/80^{+} cells were increased at Day 3 in the liver (Fig. 1C), consistent with the FACS data.

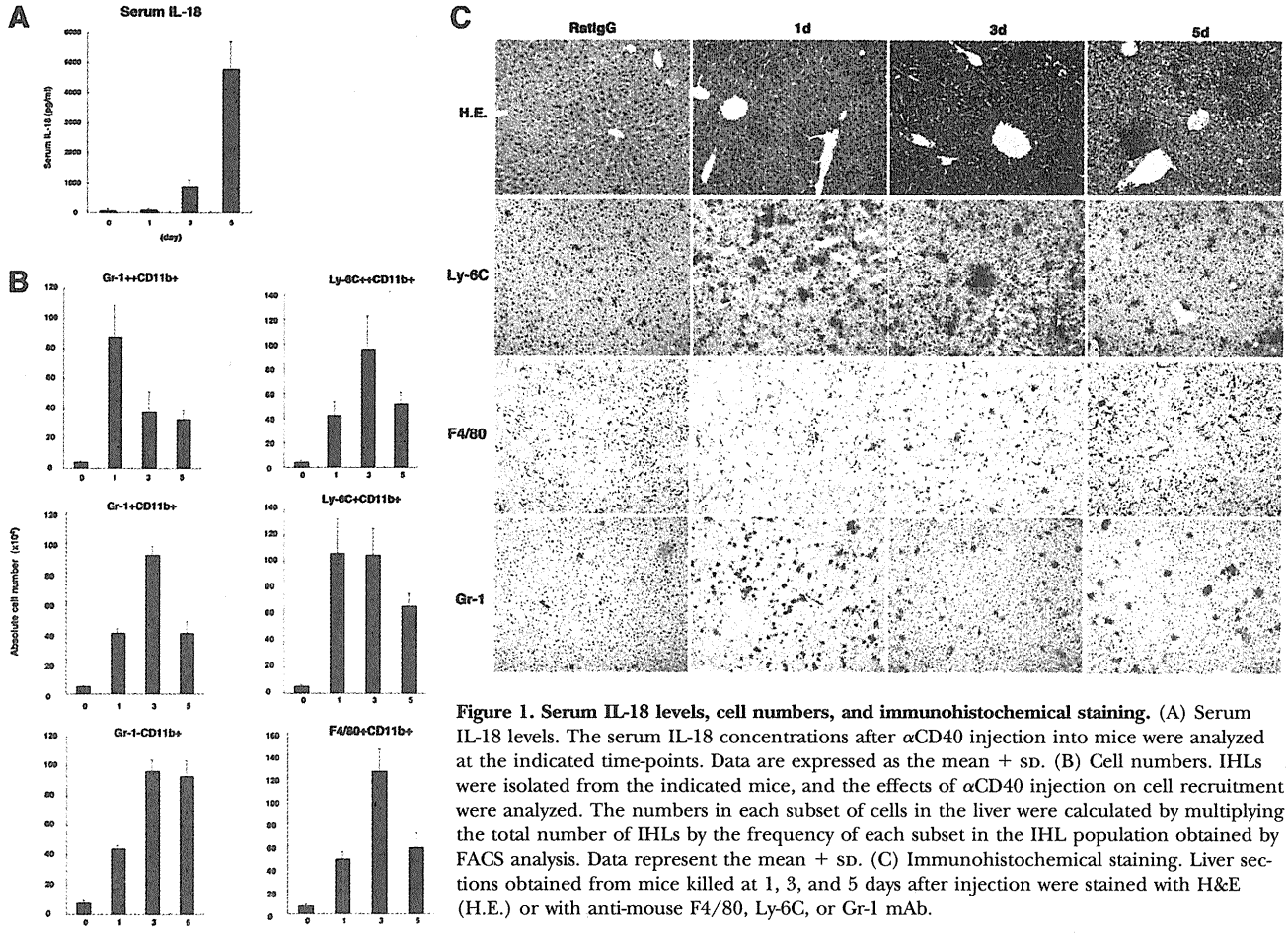

Figure 1. Serum IL-18 levels, cell numbers, and immunohistochemical staining. (A) Serum IL-18 levels. The serum IL-18 concentrations after αCD40 injection into mice were analyzed at the indicated time-points. Data are expressed as the mean + SD. (B) Cell numbers. IHLs were isolated from the indicated mice, and the effects of αCD40 injection on cell recruitment were analyzed. The numbers in each subset of cells in the liver were calculated by multiplying the total number of IHLs by the frequency of each subset in the IHL population obtained by FACS analysis. Data represent the mean + SD. (C) Immunohistochemical staining. Liver sections obtained from mice killed at 1, 3, and 5 days after injection were stained with H&E (H.E.) or with anti-mouse F4/80, Ly-6C, or Gr-1 mAb.

Proliferation and differentiation of macrophages after αCD40 injection

As reported previously [14], macrophages were key players in this liver injury. We confirmed that αCD11b mAb treatment suppressed inflammatory cytokine and chemokine expressions in the liver and the serum IL-18 levels (Supplemental Fig. 2A and B), indicating that macrophages are IL-18 producers, consistent with a previous report [11].

Next, to evaluate the function of macrophages after αCD40 injection, we analyzed the proliferation of macrophages by BrdU staining in the liver, bone marrow, and PBMCs. We injected 2 mg BrdU i.p. into mice at 2 h before sacrifice. Proliferation of $CD11b^+$ cells peaked in each tissue at Day 3 after injection and decreased by Day 5 (**Fig. 2A**), consistent with the numbers of the macrophage populations in the FACS analysis.

To determine whether differentiation from monocytes to tissue macrophages was induced in each tissue, we investigated the changes in the proportions of $Ly\text{-}6C^+$ and $F4/80^+$ cells among the $CD11b^+$ cells (Fig. 2B). $Ly\text{-}6C^-/F4/80^+/CD11b^+$ and $Ly\text{-}6C^+/F4/80^-/CD11b^+$ cells comprised the majority of cells in the liver after injection of the control antibody, and $Ly\text{-}6C^+/F4/80^+/CD11b^+$ cells increased at Day 1 and peaked at Day 3. These findings demonstrate that the proportion of $Ly\text{-}6C^-/F4/80^+/CD11b^+$ cells increased from Days 3 to 5, indicating that differentiation from monocytes to tissue macrophages had occurred by Day 3. In the bone marrow, $Ly\text{-}6C^+/F4/80^+/CD11b^+$ cells began to increase at Day 1 after αCD40 injection compared with the findings for the control antibody but had decreased by Day 5, indicating that αCD40 stimulation also induced the differentiation of macrophages. Similarly, $Ly\text{-}6C^+/F4/80^+/CD11b^+$ cells, among the PBMCs, began to increase by Day 1 after αCD40 injection and peaked at Day 3.

Role of NKT cells

To evaluate the role of NKT cells in this liver injury, NKT KO and C57BL/6 mice were injected with αCD40 and killed at Days 1 and 5. No significant difference between the serum ALT activities was observed after rat IgG injection, which is presented as Day 0, and NKT KO mice exhibited significantly lower serum ALT activities than WT mice at Days 1 and 5 ($P<0.05$; **Fig. 3A**). We also found that the absolute numbers of NK cells, T cells, macrophages, and neutrophils among the IHLs were reduced significantly in NKT KO mice (Fig. 3B). Consistent with the reduced number of IHLs in NKT KO mice, the IFN-γ, TNF-α, CCL2, and CCL5 mRNA expressions in the liver were suppressed at Days 1 and 5 after αCD40 injection (Fig. 3C and

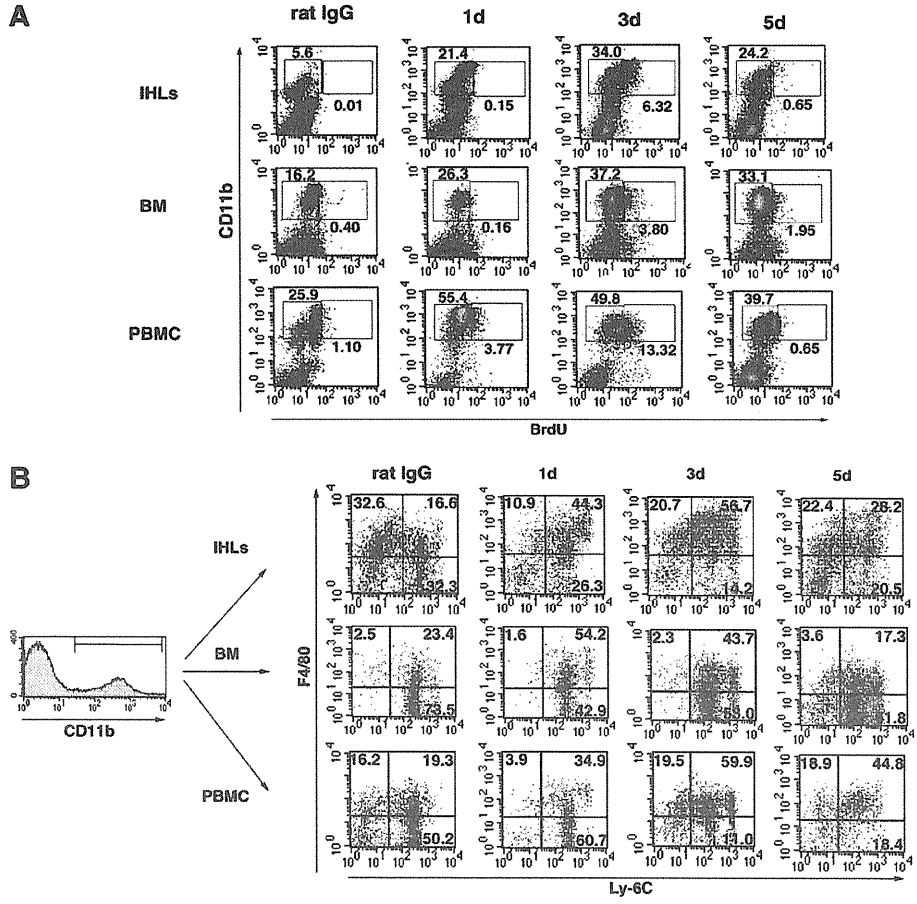

Figure 2. Macrophage differentiation and proliferation after αCD40 injection. (A) To analyze macrophage proliferation in IHLs, bone marrow (BM), and PBMCs after αCD40 injection, C57BL/6 mice were injected i.p. with 2 mg BrdU at 2 h before sacrifice. Cells were stained with anti-CD11b-allophycocyanin and anti-BrdU-FITC antibodies. (B) To analyze macrophage differentiation in IHLs, bone marrow, and PBMCs, cells were stained with anti-CD11b-allophycocyanin, anti-mouse F4/80-FITC, and anti-mouse Ly-6C-PE mAb.

D). We further found that the IFN-γ production by NK cells and TNF-α production by macrophages were suppressed in NKT KO mice (**Supplemental Fig. 3**). Furthermore, the serum IL-18 levels were reduced in NKT KO mice at Day 5 but not Day 1.

Finally, the numbers of Ly-6C^{++}/CD11b^{+}, Ly-6C^{+}/CD11b^{+}, and F4/80^{+}/CD11b^{+} cells in NKT KO mice were reduced significantly compared with WT mice at Day 5 after injection (Fig. 3E), demonstrating that NKT cells were involved in the macrophage and monocyte infiltration in the liver.

Depletion of neutrophils exacerbates the liver injury

To determine whether neutrophils play a role in this liver injury, we injected αCD40 into C57BL/6 mice with αGr-1 mAb or rat IgG2b at Days −1, +1, and +3. The mice were killed at Day 5. We confirmed that αGr-1 mAb treatment specifically depleted IHLs with an efficiency of >95% (Gr-1^{++}/CD11b^{+} cells), as evaluated by FACS analysis (Supplemental Fig. 4).

Administration of αGr-1 mAb significantly increased the serum ALT activity at Day 5 compared with the control antibody (P<0.05; **Fig. 4A**). Although the total number of IHLs decreased after αCD40 plus αGr-1 mAb treatment, the numbers of Gr-1^{+}/CD11b^{+} cells, including Ly-6C^{++}/CD11b^{+} and F4/80^{+}/CD11b^{+} cells, increased (Fig. 4B, C, and E). Immunohistochemical analyses revealed that Ly-6C^{+} and F4/80^{+} cells were increased in the liver at Day 5 after αCD40 mAb plus αGr-1 mAb treatment (Fig. 4F). Consistent with these observations, the serum TNF-α and IL-18 but not IFN-γ levels were elevated in the neutrophil-depleted state (Fig. 4D). In addition, TNF-α production by Ly-6C^{++}/CD11b^{+} and F4/80^{+}/CD11b^{+} cells was increased in αGr-1 mAb-treated mice (Fig. 4G), suggesting that neutrophils may play a suppressive role in macrophage recruitment and function in this liver inflammation.

Neutralization of IL-18 suppresses the liver injury

To assess whether IL-18 is responsible for the αCD40-induced liver injury, we injected C57BL/6 mice with αIL-18 mAb or rat IgG as a control at –1, +1, and 2 days after αCD40 injection and then killed the mice at Day 5. Administration of αIL-18 mAb significantly suppressed the serum ALT activity at Day 5 (P<0.05; **Fig. 5A**), demonstrating that IL-18 contributes to the liver injury. Consistent with this finding, αIL-18 mAb treatment decreased the IFN-γ and TNF-α mRNA expressions in the liver (Fig. 5B). We also found that αIL-18 mAb treatment inhibited the recruitment of macrophage subpopulations, neutrophils, NK cells, and T cells but not NKT cells into the liver (Fig. 5C). Immunohistochemical analyses revealed that Ly-6C^{+} and F4/80^{+} cells

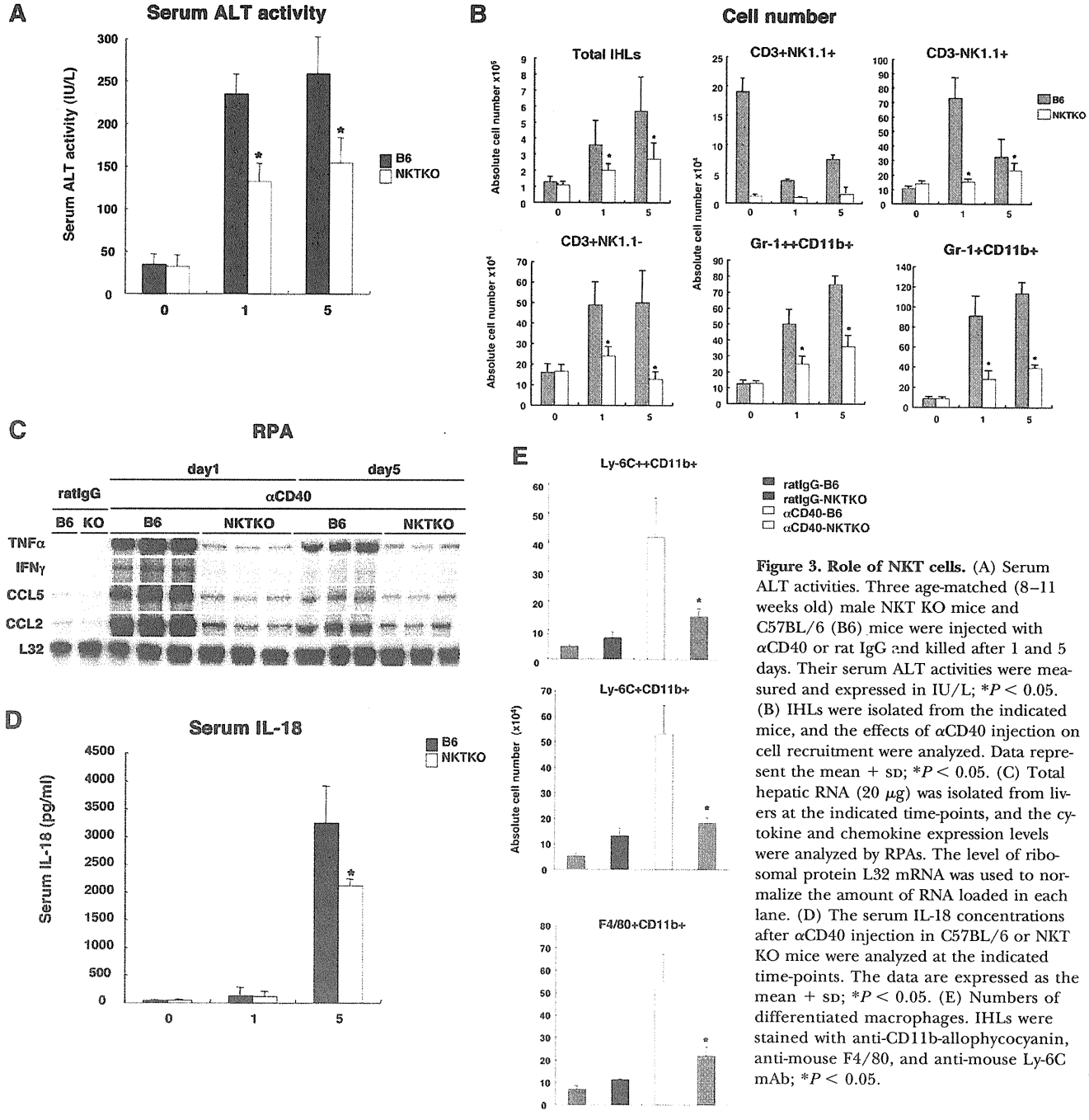

Figure 3. Role of NKT cells. (A) Serum ALT activities. Three age-matched (8–11 weeks old) male NKT KO mice and C57BL/6 (B6) mice were injected with αCD40 or rat IgG and killed after 1 and 5 days. Their serum ALT activities were measured and expressed in IU/L; $*P < 0.05$. (B) IHLs were isolated from the indicated mice, and the effects of αCD40 injection on cell recruitment were analyzed. Data represent the mean + SD; $*P < 0.05$. (C) Total hepatic RNA (20 μg) was isolated from livers at the indicated time-points, and the cytokine and chemokine expression levels were analyzed by RPAs. The level of ribosomal protein L32 mRNA was used to normalize the amount of RNA loaded in each lane. (D) The serum IL-18 concentrations after αCD40 injection in C57BL/6 or NKT KO mice were analyzed at the indicated time-points. The data are expressed as the mean + SD; $*P < 0.05$. (E) Numbers of differentiated macrophages. IHLs were stained with anti-CD11b-allophycocyanin, anti-mouse F4/80, and anti-mouse Ly-6C mAb; $*P < 0.05$.

were decreased in the liver at Day 5 after αCD40 mAb plus αIL-18 mAb treatment (Fig. 5D).

IL-18 causes severe liver injury with high levels of IFN-γ

To evaluate the effect of IL-18 on the late-phase liver injury, we i.p.-injected mice with 1 μg murine rIL-18 at 4 days after αCD40 injection and measured their serum ALT activity and inflammatory cytokine levels. The serum ALT activity was increased significantly by about four times after rIL-18 treatment compared with the control, although the number of IHLs, except for the macrophage population, was suppressed (**Fig. 6A–C**). In addition, serum IFN-γ was elevated significantly after injection of αCD40 with rIL-18, and NK cells strongly produced IFN-γ after rIL-18 treatment (Fig. 6D and E). In contrast, no difference was seen for TNF-α production by macrophages (Fig. 6E). Thus, IL-18 mainly activated NK cells and reduced the numbers of monocytes and neutrophils in the liver (Fig. 6A and B).

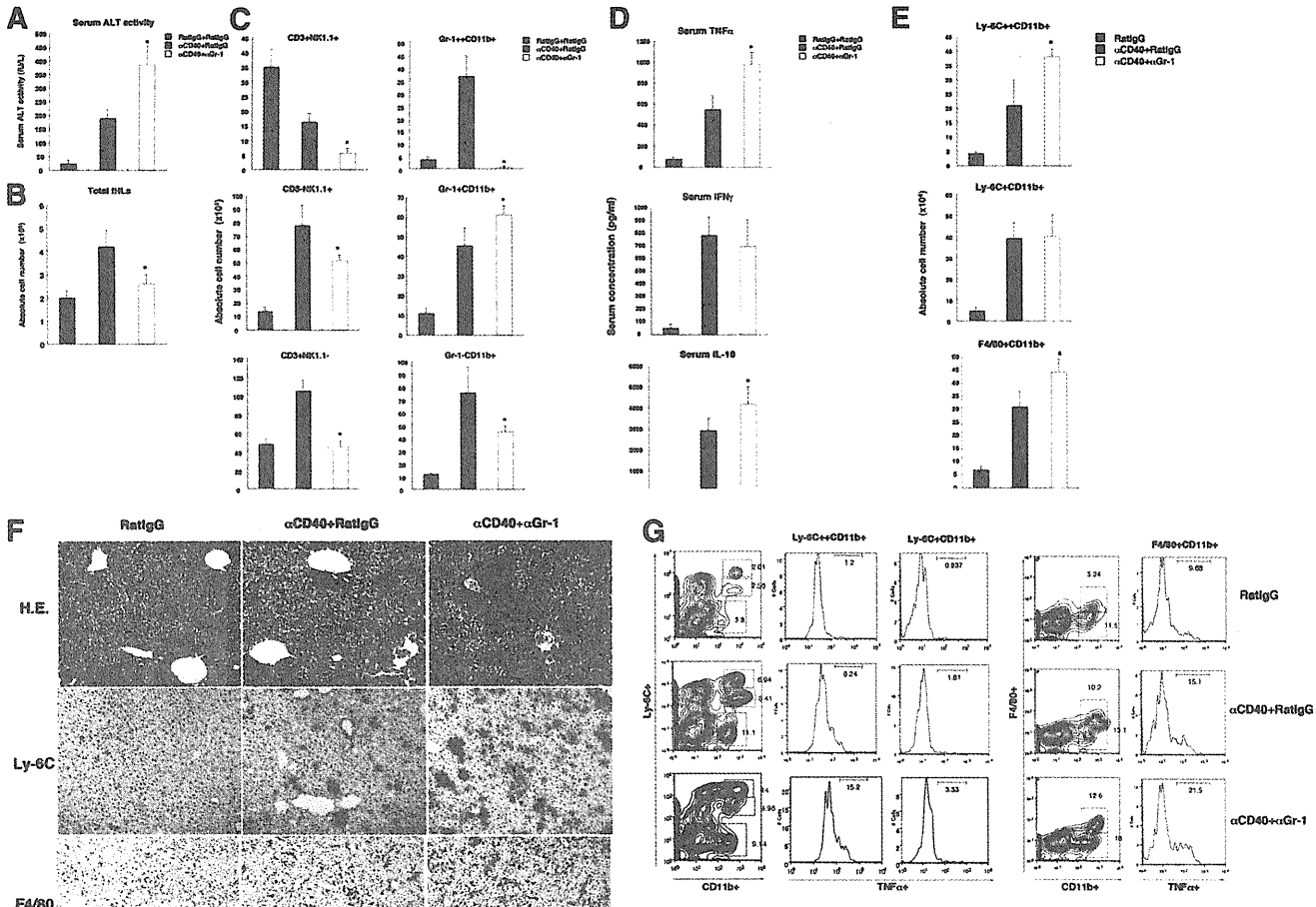

Figure 4. Role of neutrophils. (A) Serum ALT activities. C57BL/6 mice were injected with αCD40 or rat IgG in the absence or presence of αGr-1 mAb and killed after 5 days. Their serum ALT activities were measured and expressed in IU/L; $*P < 0.05$. (B and C) IHLs were isolated from the indicated mice, and the effects of αGr-1 mAb on cell recruitment were analyzed. Data represent the mean + SD; $*P < 0.05$. (D) Serum cytokine concentrations after αCD40 injection in C57BL/6 mice. Data are expressed as the mean + SD; $*P < 0.05$. (E) Numbers of differentiated macrophages. IHLs were stained with anti-CD11b-allophycocyanin, anti-mouse F4/80, and anti-mouse Ly-6C mAb; $*P < 0.05$. (F) Immunohistochemical staining. Liver sections obtained from mice killed at 5 days after injection were stained with H&E or with anti-mouse F4/80, Ly-6C, or Gr-1 mAb. (G) Intracellular cytokine expression levels in macrophages and monocytes. To determine which cell populations produced TNF-α after injection, we stained the cells with anti-mouse F4/80-FITC, Ly-6C-PE, anti-CD11b-allophycocyanin, and anti-TNF-α-PE mAb. The cells were analyzed using a FACSCalibur system.

DISCUSSION

The present study has clarified several important aspects of liver pathology in terms of inflammatory cell recruitment and activation in the liver and provides important findings regarding the interactions among IL-18, macrophages, neutrophils, and NKT cells. The innate immune system, which is considered to provide nonantigen-specific immune responses, can provide emergency signals from destroyed hepatocytes during liver inflammation, resulting in an inflammatory response. These inflammatory events contribute to liver injury and conversely, may also be involved in liver repair based on various experimental liver disease models [18–20]. Therefore, it is well established that an inflammatory response is essential for controlling the microenvironment in the liver, but the relationships among macrophages and other inflammatory cells with regard to liver injury are still obscure. Careful interpretation is required to evaluate the results of the present study, especially with regard to the interactions between IHLs and the liver injury in this model. The liver injury model that we used involves artificial stimulation of macrophages, monocytes, and B cells that express CD40, and these cells subsequently activate NK cells and NKT cells, thereby causing liver injury by way of IFN-γ, TNF-α, and IL-12 [14, 15]. In general, it has

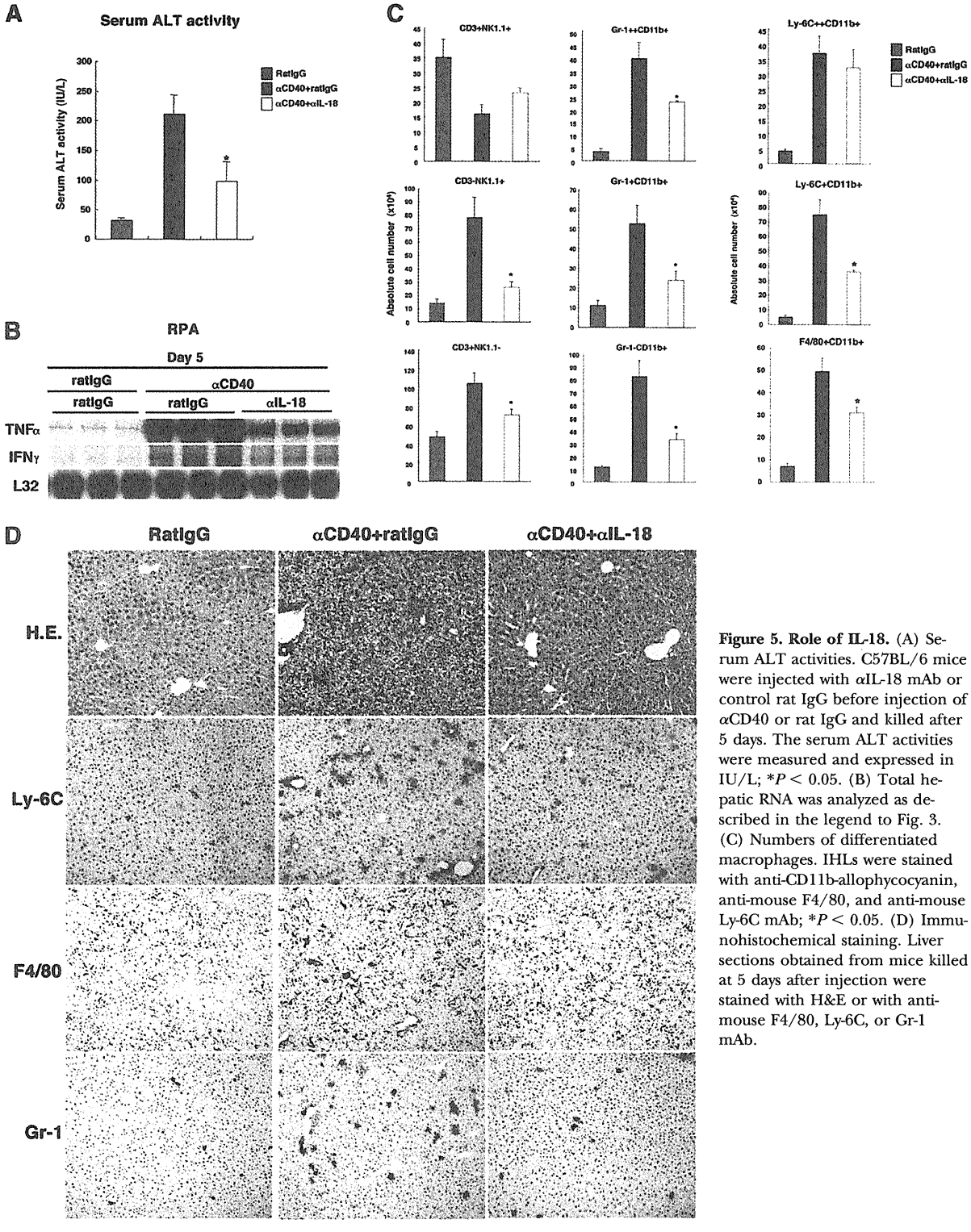

Figure 5. Role of IL-18. (A) Serum ALT activities. C57BL/6 mice were injected with αIL-18 mAb or control rat IgG before injection of αCD40 or rat IgG and killed after 5 days. The serum ALT activities were measured and expressed in IU/L; $*P < 0.05$. (B) Total hepatic RNA was analyzed as described in the legend to Fig. 3. (C) Numbers of differentiated macrophages. IHLs were stained with anti-CD11b-allophycocyanin, anti-mouse F4/80, and anti-mouse Ly-6C mAb; $*P < 0.05$. (D) Immunohistochemical staining. Liver sections obtained from mice killed at 5 days after injection were stained with H&E or with anti-mouse F4/80, Ly-6C, or Gr-1 mAb.

been well understood that the interactions between CD40 and CD40 ligand reciprocally deliver activating signals to APCs and cognate T cells. This process is critically important for the development of adaptive immunity [21–23]. However, we consider that this liver injury model is useful for analyzing how activated macrophages or B cells affect the activation of other IHLs and their recruitment in liver injury, as the agonistic CD40 antibody mainly activates macrophages and B cells.

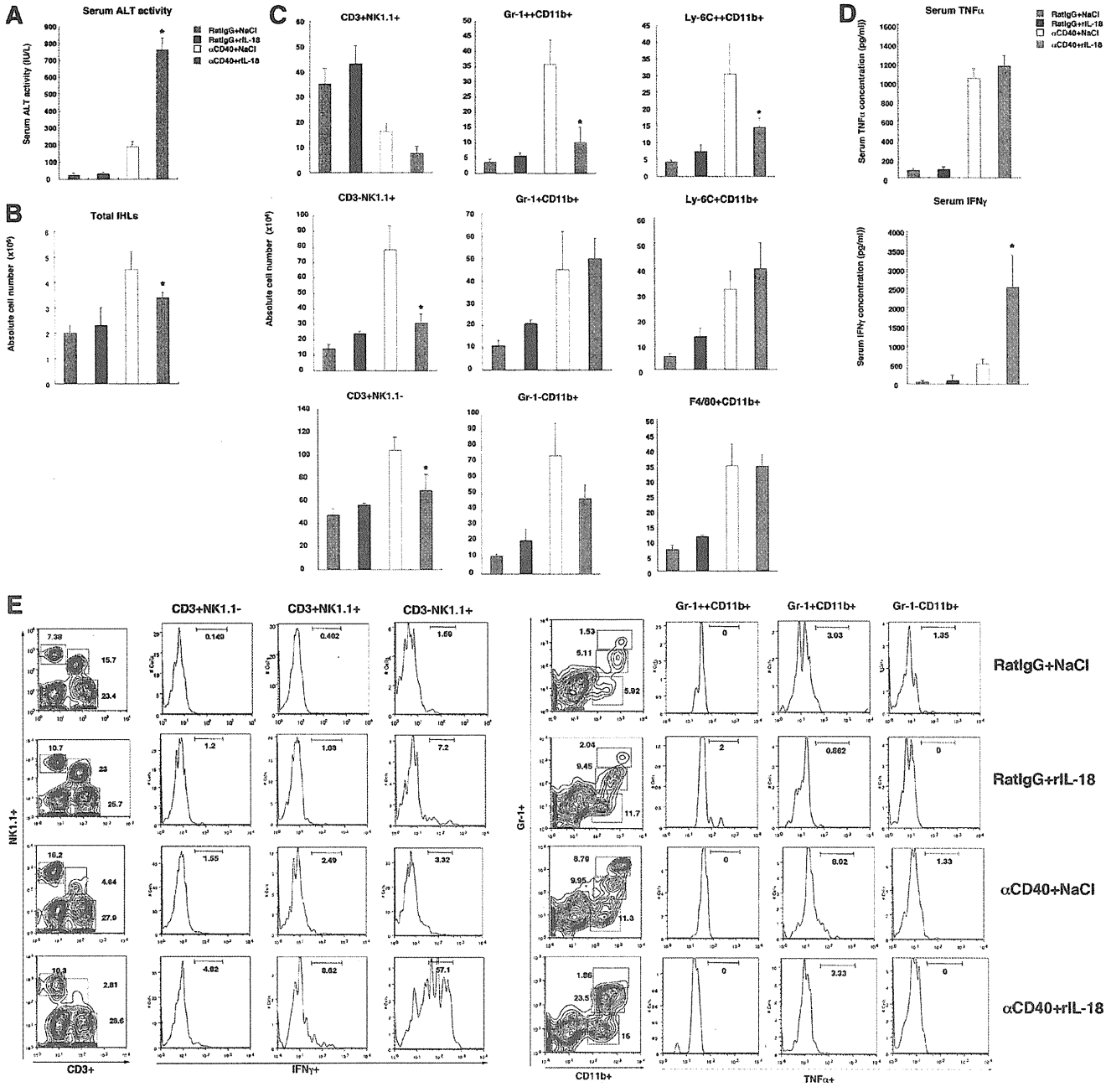

Figure 6. Additional IL-18 treatment exacerbates liver injury after αCD40 injection. (A) Serum ALT activities. C57BL/6 mice were injected with αCD40 or rat IgG in the absence or presence of rIL-18 and killed after 5 days. The serum ALT activities were measured and expressed in IU/L; $^*P < 0.05$. (B and C) IHLs were isolated from the indicated mice, and the effects of IL-18 on cell recruitment were analyzed. Data represent the mean + SD; $^*P < 0.05$. (D) Serum cytokine concentrations after αCD40 injection in C57BL/6 mice. Data are expressed as the mean + SD; $^*P < 0.05$. (E) Intracellular cytokine expression levels in macrophages and monocytes. To determine which cell populations produced TNF-α after injection, we stained the cells with anti-mouse F4/80-FITC, Ly-6C-PE, anti-CD11b-allophycocyanin, and anti-TNF-α-PE mAb. The cells were analyzed using a FACSCalibur system.

First, we determined the characteristics of intrahepatic macrophages, which became activated on Days 1 and 5 after αCD40 injection, as they are key effector cells for the liver injury [14]. We analyzed the proliferation of the macrophages and detected a peak at Day 3. This finding was consistent with the observed numbers of macrophages. Notably, the highly proliferating macrophages were unable to produce TNF-α, and this is considered to be one of the reasons why αCD40-triggered inflammation exhibits a biphasic pattern in the liver. The present study demonstrated that monocyte subsets differing in Ly-6C expression represented different stages in

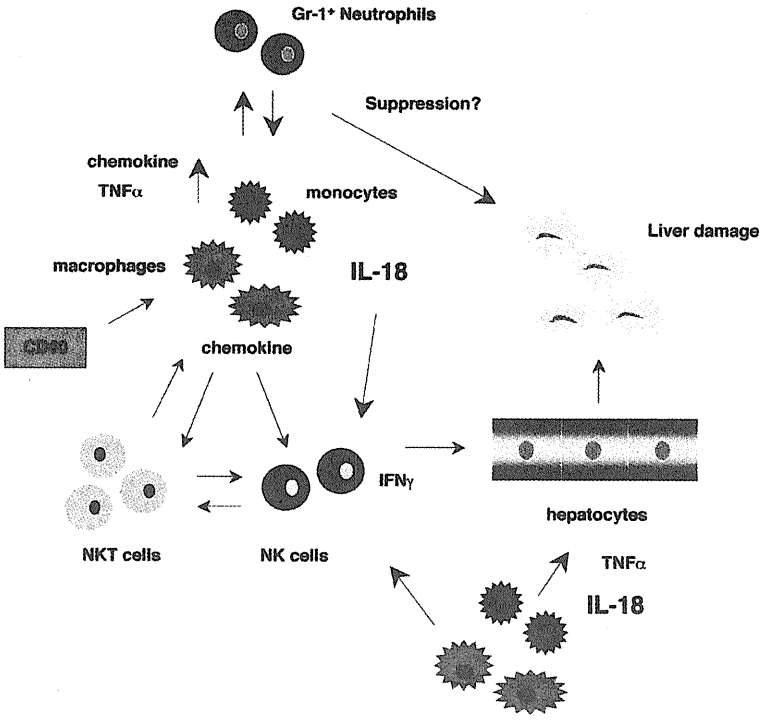

Figure 7. Scheme for how αCD40 triggers liver inflammation. 1) TNF-α and chemokines are produced by activated macrophages after αCD40 stimulation. 2) Neutrophils increase rapidly and control the activation of macrophages or monocytes. 3) At the same time, NKT cells are activated and produce inflammatory cytokines. 4) IL-18 stimulates the migration of macrophages and monocytes into the liver and activates NK cells. 5) Inflammatory cytokines stimulate IFN-γ production by NK cells, and the produced IFN-γ further stimulates macrophages and exacerbates the severe liver injury.

a continuous maturation pathway, and previous in vitro experiments indicated that this transition occurs within 24–48 h [24]. Based on these findings, we suggest that not only the increase in Ly-6C^{high} monocytes, which have suppressive functions [25], but also the high proliferation of macrophages may cause the suppressed inflammatory response at Day 3. Although we investigated the suppressive inflammatory cytokine IL-10, we were unable to confirm the elevated production of this cytokine in the liver at Day 3 compared with Day 5 (Supplemental Fig. 1).

Although tissue macrophages and monocytes increased to reach a peak at Day 3 after injection, neutrophils increased rapidly and were reduced by Day 3. Interestingly, we found that neutrophil depletion exacerbated the αCD40-induced liver injury. In general, neutrophils have an effector function against several liver injury models, such as those involving carbon tetrachloride- and ischemic/perfusion-induced liver injury [26, 27]. These previous studies demonstrated that reactive oxygen from neutrophils is a key factor for hepatocyte damage. Our findings seem to be contradictory to the well-established paradigm that neutrophils induce tissue damage. However, the outcomes of αGr-1 treatment may vary depending on the liver injury models involved, as we have shown already that αGr-1 treatment partially protects against liver injury in hepatitis B virus transgenic mice [28, 29].

A recent report suggested that Gr-1^{high}CD11b^{+} cells suppress T cells in tumor-bearing mice [30] and that Gr-1^{high}CD11b^{low} polymononuclear cell–myeloid-derived suppressor cell populations have suppressive potential in the healthy spleen [31]. These reports suggest the possibility that liver injury is exacerbated by depletion of suppressive, Gr-1-positive cells. Furthermore, we need to confirm whether antibody-tagged neutrophils accumulate in the liver and whether Kupffer cells are activated by phagocytosis. In fact, we found that αGr-1 treatment induced the migration of macrophages and monocytes into the liver, and these cells produced large amounts of TNF-α, indicating that conclusive evidence for whether neutrophils have suppressive effects on this liver injury may require further investigations.

We further found that NKT cells participated in the αCD40-induced biphasic liver injury. NKT cells are particularly abundant in the liver, accounting for 20–30% of IHLs, and are thought to play roles in immunity against intracellular bacteria and parasites and certain tumors [8, 32]. It is well established that CD40 cross-linking induces DCs to up-regulate their expressions of CD40, B7.1, B7.2, and IL-12, which in turn, enhance NKT cell activation and cytokine production [32]. In this liver injury, NKT cells activated other inflammatory cells, including NK cells and macrophages, in the liver, as IFN-γ production by NK cells and TNF-α production by macrophages were apparently blocked in the liver of NKT KO mice. Consistent with the finding that macrophage recruitment was reduced in NKT KO mice, infiltration of the various macrophage subpopulations was also inhibited, indicating that NKT cells have an influence on macrophage differentiation following αCD40 injection. It is of note that NKT cells were secondarily activated by way of CD40 ligation on macrophages and DCs and that NKT KO mice appear to exhibit protection against inflammatory cell recruitment into the liver. These findings demonstrate the importance of NKT cells for the propagation of inflammatory liver disease.

In this study, we have demonstrated that IL-18 is involved in the late-phase liver injury. Although we found that IL-12 played a pivotal role in the early-phase liver injury, IL-18 was not necessary for liver injury to occur, as neutralization of IL-18 did not increase the serum ALT activity (Supplemental Fig. 5). IL-18 is known to induce NK and NKT cells to produce IFN-γ [12], but it

requires IL-12 to induce IFN-γ production by Th1 cells [11]. In keeping with these findings, we found that rIL-18 treatment rapidly induced intrahepatic NK cells to produce large amounts of IFN-γ and also to cause severe liver injury. Importantly, these effects did not involve TNF-α and did not require the recruitment of macrophages, monocytes, and neutrophils into the liver. More recently, intracellular microbial sensors have been identified, including NLRs [33, 34]. Some of the NLRs also sense nonmicrobial danger signals and form large cytoplasmic complexes called inflammasomes, which link the sensing of microbial products and metabolic stress to proteolytic activation of the proinflammatory cytokines IL-1β and IL-18. Therefore, in this model, the danger signals for early liver damage may trigger the activation of inflammasomes, resulting in the production of IL-18 and subsequent induction of liver damage.

In conclusion, the present results demonstrate that activation of intrahepatic macrophages can initiate a cascade of events that begins with the production of inflammatory cytokines and chemokines and leads to the activation of intrahepatic NK and NKT cells for the production of IFN-γ, all of which contribute to the recruitment of additional inflammatory cells to the liver (**Fig. 7**). We have shown that the interactions among macrophages, monocytes, neutrophils, and NKT cells participate efficiently and closely in the exacerbation of liver inflammation through cytokine and chemokine production. Further studies are required to identify the roles of the suppressive monocyte or neutrophil subpopulations in the liver injury, and clarification of the roles of these cell types will be useful in the treatment of various liver diseases.

AUTHORSHIP

K.K. planned the experimental project, and K.K., S.S., S.H., Y.H., T.H., and M.N. performed data analysis and wrote the paper. M.K. contributed data and comments about the manuscript.

ACKNOWLEDGMENTS

This study was supported by a grant-in-aid (B) from the Ministry of Education, Culture, Sports, Science and Technology of Japan (grant no. 20390203) and a grant-in-aid for specially promoted research on viral diseases from the Tokyo Metropolitan Government to K.K. We thank Dr. Francis V. Chisari (The Scripps Research Institute) for supporting this study and Dr. Antonius Rolink (Basel Institute for Immunology) for providing the anti-mouse agonistic CD40 mAb. We are also grateful to Drs. Toshinori Nakayama (Chiba University) and Masaru Taniguchi (RIKEN) for providing the Vα14 NKT KO mice.

REFERENCES

1. Akira, S., Uematsu, S., Takeuchi, O. (2006) Pathogen recognition and innate immunity. *Cell* **124,** 783–801.
2. Crispe, I. N. (2009) The liver as a lymphoid organ. *Annu. Rev. Immunol.* **27,** 147–163.
3. Crispe, I. N. (2003) Hepatic T cells and liver tolerance. *Nat. Rev. Immunol.* **3,** 51–62.
4. Banchereau, J., Briere, F., Caux, C., Davoust, J., Lebecque, S., Liu, Y. J., Pulendran, B., Palucka, K. (2000) Immunobiology of dendritic cells. *Annu. Rev. Immunol.* **18,** 767–811.
5. Munder, M., Mallo, M., Eichmann, K., Modolell, M. (1998) Murine macrophages secrete interferon γ upon combined stimulation with interleukin (IL)-12 and IL-18: a novel pathway of autocrine macrophage activation. *J. Exp. Med.* **187,** 2103–2108.
6. Zlotnik, A., Yoshie, O. (2000) Chemokines: a new classification system and their role in immunity. *Immunity* **12,** 121–127.
7. Wardle, E. N. (1987) Kupffer cells and their function. *Liver* **7,** 63–75.
8. Taniguchi, M., Harada, M., Kojo, S., Nakayama, T., Wakao, H. (2003) The regulatory role of Vα14 NKT cells in innate and acquired immune response. *Annu. Rev. Immunol.* **21,** 483–513.
9. Seino, K., Taniguchi, M. (2005) Functionally distinct NKT cell subsets and subtypes. *J. Exp. Med.* **202,** 1623–1626.
10. Van Kaer, L., Joyce, S. (2005) Innate immunity: NKT cells in the spotlight. *Curr. Biol.* **15,** R429–R431.
11. Nakanishi, K., Yoshimoto, T., Tsutsui, H., Okamura, H. (2001) Interleukin-18 regulates both Th1 and Th2 responses. *Annu. Rev. Immunol.* **19,** 423–474.
12. Okamura, H., Kashiwamura, S., Tsutsui, H., Yoshimoto, T., Nakanishi, K. (1998) Regulation of interferon-γ production by IL-12 and IL-18. *Curr. Opin. Immunol.* **10,** 259–264.
13. Kimura, K., Kakimi, K., Wieland, S., Guidotti, L. G., Chisari, F. V. (2002) Interleukin-18 inhibits hepatitis B virus replication in the livers of transgenic mice. *J. Virol.* **76,** 10702–10707.
14. Kimura, K., Kakimi, K., Wieland, S., Guidotti, L. G., Chisari, F. V. (2002) Activated intrahepatic antigen-presenting cells inhibit hepatitis B virus replication in the liver of transgenic mice. *J. Immunol.* **169,** 5188–5195.
15. Kimura, K., Moriwaki, H., Nagaki, M., Saio, M., Nakamoto, Y., Naito, M., Kuwata, K., Chisari, F. V. (2006) Pathogenic role of B cells in anti-CD40-induced necroinflammatory liver disease. *Am. J. Pathol.* **168,** 786–795.
16. Rolink, A., Melchers, F., Andersson, J. (1996) The SCID but not the RAG-2 gene product is required for S μ-S ε heavy chain class switching. *Immunity* **5,** 319–330.
17. Naito, M., Nagai, H., Kawano, S., Umezu, H., Zhu, H., Moriyama, H., Yamamoto, T., Takatsuka, H., Takei, Y. (1996) Liposome-encapsulated dichloromethylene diphosphonate induces macrophage apoptosis in vivo and in vitro. *J. Leukoc. Biol.* **60,** 337–344.
18. Gao, B., Jeong, W. I., Tian, Z. (2008) Liver: an organ with predominant innate immunity. *Hepatology* **47,** 729–736.
19. Guidotti, L. G., Chisari, F. V. (2001) Noncytolytic control of viral infections by the innate and adaptive immune response. *Annu. Rev. Immunol.* **19,** 65–91.
20. Jaeschke, H., Bajt, M. L. (2004) Critical role of CXC chemokines in endotoxemic liver injury in mice. *J. Leukoc. Biol.* **76,** 1089–1090, author reply 1091–1092.
21. Banchereau, J., Bazan, F., Blanchard, D., Briere, F., Galizzi, J. P., van Kooten, C., Liu, Y. J., Rousset, F., Saeland, S. (1994) The CD40 antigen and its ligand. *Annu. Rev. Immunol.* **12,** 881–922.
22. Cella, M., Scheidegger, D., Palmer-Lehmann, K., Lane, P., Lanzavecchia, A., Alber, G. (1996) Ligation of CD40 on dendritic cells triggers production of high levels of interleukin-12 and enhances T cell stimulatory capacity: T-T help via APC activation. *J. Exp. Med.* **184,** 747–752.
23. Grewal, I. S., Flavell, R. A. (1998) CD40 and CD154 in cell-mediated immunity. *Annu. Rev. Immunol.* **16,** 111–135.
24. Leenen, P. J., de Bruijn, M. F., Voerman, J. S., Campbell, P. A., van Ewijk, W. (1994) Markers of mouse macrophage development detected by monoclonal antibodies. *J. Immunol. Methods* **174,** 5–19.
25. Zhu, B., Bando, Y., Xiao, S., Yang, K., Anderson, A. C., Kuchroo, V. K., Khoury, S. J. (2007) CD11b+Ly-6C(hi) suppressive monocytes in experimental autoimmune encephalomyelitis. *J. Immunol.* **179,** 5228–5237.
26. Duffield, J. S., Forbes, S. J., Constandinou, C. M., Clay, S., Partolina, M., Vuthoori, S., Wu, S., Lang, R., Iredale, J. P. (2005) Selective depletion of macrophages reveals distinct, opposing roles during liver injury and repair. *J. Clin. Invest.* **115,** 56–65.
27. Luster, M. I., Simeonova, P. P., Gallucci, R. M., Bruccoleri, A., Blazka, M. E., Yucesoy, B. (2001) Role of inflammation in chemical-induced hepatotoxicity. *Toxicol. Lett.* **120,** 317–321.
28. Takai, S., Kimura, K., Nagaki, M., Satake, S., Kakimi, K., Moriwaki, H. (2005) Blockade of neutrophil elastase attenuates severe liver injury in hepatitis B transgenic mice. *J. Virol.* **79,** 15142–15150.
29. Sitia, G., Isogawa, M., Kakimi, K., Wieland, S. F., Chisari, F. V., Guidotti, L. G. (2002) Depletion of neutrophils blocks the recruitment of antigen-nonspecific cells into the liver without affecting the antiviral activity of hepatitis B virus-specific cytotoxic T lymphocytes. *Proc. Natl. Acad. Sci. USA* **99,** 13717–13722.
30. Dolcetti, L., Peranzoni, E., Ugel, S., Marigo, I., Fernandez Gomez, A., Mesa, C., Geilich, M., Winkels, G., Traggiai, E., Casati, A., Grassi, F., Bronte, V. (2010) Hierarchy of immunosuppressive strength among myeloid-derived suppressor cell subsets is determined by GM-CSF. *Eur. J. Immunol.* **40,** 22–35.
31. Greifenberg, V., Ribechini, E., Rossner, S., Lutz, M. B. (2009) Myeloid-derived suppressor cell activation by combined LPS and IFN-γ treatment impairs DC development. *Eur. J. Immunol.* **39,** 2865–2876.
32. Kronenberg, M. (2005) Toward an understanding of NKT cell biology: progress and paradoxes. *Annu. Rev. Immunol.* **23,** 877–900.
33. Martinon, F., Mayor, A., Tschopp, J. (2009) The inflammasomes: guardians of the body. *Annu. Rev. Immunol.* **27,** 229–265.
34. Pétrilli, V., Dostert, C., Muruve, D. A., Tschopp, J. (2007) The inflammasome: a danger sensing complex triggering innate immunity. *Curr. Opin. Immunol.* **19,** 615–622.

KEY WORDS:
neutrophil · macrophage · NKT cell · chemokine · IL-18

Journal of Medical Virology 83:801–809 (2011)

Translocase of Outer Mitochondrial Membrane 70 Expression Is Induced by Hepatitis C Virus and Is Related to the Apoptotic Response

Takashi Takano,[1,2,3] Michinori Kohara,[2] Yuri Kasama,[1] Tomohiro Nishimura,[1,4] Makoto Saito,[1] Chieko Kai,[3] and Kyoko Tsukiyama-Kohara[1]*

[1]*Faculty of Life Sciences, Department of Experimental Phylaxiology, Kumamoto University, Kumamoto, Japan*
[2]*Department of Microbiology and Cell Biology, Tokyo Metropolitan Institute of Medical Science, Tokyo, Japan*
[3]*Laboratory Animal Research Center, Institute of Medical Science, The University of Tokyo, Tokyo, Japan*
[4]*The Chemo-Sero-Therapeutic Research Institute, Kikuchi Research Center, Kyokushi, Kikuchi, Kumamoto, Japan*

The localization of hepatitis C virus (HCV) proteins in cells leads to several problems. The translocase of outer mitochondrial membrane 70 (TOM70) is a mitochondrial import receptor. In this study, TOM70 expression was induced by HCV infection. TOM70 overexpression induced resistance to tumor necrosis factor-alpha (TNF-α)-mediated apoptosis but not to Fas-induced apoptosis in HepG2 cells. TOM70 was found to be induced by the HCV non-structural protein (NS)3/4A protein, and silencing of TOM70 decreased the levels of the NS3 and Mcl-1 proteins. These results indicate that TOM70 can directly interact with the NS3 protein. In hepatoma cells, silencing of TOM70 induced apoptosis and increased caspase-3/7 activity but did not modify caspase-8 and caspase-9 activity. TOM70 silencing-induced apoptosis was impaired in HCV NS3/4A protein-expressing cells. Thus, this study revealed a novel finding, that is, TOM70 is linked with the NS3 protein and the apoptotic response. ***J. Med. Virol. 83:801–809, 2011.***

KEY WORDS: hepatitis C virus; translocase of outer mitochondrial membrane 70; apoptosis; non-structural protein 3; tumor necrosis factor-alpha

INTRODUCTION

Hepatitis C virus (HCV) infection causes acute and chronic hepatitis, cirrhosis, and hepatocellular carcinoma (HCC) [Seeff, 2002]. HCV easily establishes chronic infection, and localization of HCV proteins is reported to induce several disturbances in cells. One of the major target organelles of HCV is the mitochondrion, and HCV non-structural protein (NS)3/4A protease cleaves the mitochondrial antiviral signaling (MAVS)/IPS-1/VISA/Cardif protein, thereby impairing interferon signaling [Li et al., 2005] and influencing apoptotic responses [Nomura-Takigawa et al., 2006; Deng et al., 2008; Lei et al., 2009].

Most mitochondrial proteins are synthesized in the cytosol as preproteins, targeted to the mitochondria by cytosolic factors such as HSP70 and mitochondrial import stimulation factor (MSF), and transported to the intramitochondrial compartments by the preprotein import machineries of the outer and inner membranes (TOM and TIM complexes, respectively) [Mihara and Omura, 1996; Schatz, 1996; Neupert, 1997; Pfanner and Meijer, 1997]. The TOM machinery consists of two import receptors, namely, TOM20 and TOM70, and several other subunits that are arranged in a tightly bound complex termed the general import pore [Pfanner and Geissler, 2001; Hoogenraad et al., 2002; Stojanovski et al., 2003]. TOM70 was identified in *Saccharomyces cerevisiae* as a 70-kDa protein with no known function [Truscott et al., 2001]. TOM70 is recognized as the primary receptor for proteins with internal targeting signals, such as the F_1-ATPase β-subunit

Additional Supporting Information may be found in the online version of this article.

Grant sponsor: Ministry of Health and Welfare of Japan; Grant sponsor: Clinical and Epidemiological Studies of Emerging and Re-emerging Infectious Diseases (Cooperative Research Project).

Takashi Takano present address is Division of Veterinary Public Health, Nippon Veterinary and Life Science University, 1-7-1 Kyonan, Musashino, Tokyo 180-8602, Japan.

*Correspondence to: Kyoko Tsukiyama-Kohara, Faculty of Life Sciences, Department of Experimental Phylaxiology, Kumamoto University, 1-1-1 Honjo, Kumamoto 860-8556, Japan.
E-mail: kkohara@kumamoto-u.ac.jp

Accepted 13 December 2010
DOI 10.1002/jmv.22046
Published online in Wiley Online Library (wileyonlinelibrary.com).

and cytochrome c_1 [Truscott et al., 2001]. TOM70 interacts with human myeloid cell leukemia-1 (Mcl-1), a Bcl-2 family member, and this interaction facilitates the mitochondrial targeting of Mcl-1 [Chou et al., 2006]. Mcl-1 can interact with the HCV core protein and suppresses core-induced apoptosis [Mohd-Ismail et al., 2009].

In the present study, it was found that TOM70 activity was enhanced by HCV. This study addresses TOM70 modification by HCV and its role in the apoptotic response.

MATERIALS AND METHODS

Cells

WRL68, HepG2, HuH-7, and HepG2 cells expressing non-structural proteins (Lenti-NS3/4A-HepG2, Lenti-NS4B-HepG2, Lenti-NS5A-HepG2, Lenti-NS5B-HepG2, and Lenti-empty-HepG2) were maintained and established as described previously [Tsukiyama-Kohara et al., 2004; Nishimura et al., 2009; Saitou et al., 2009]. The Cre/loxP conditional expression system for full-length HCV cDNA (*HCR6-Rz*) in RzM6 cells [Tsukiyama-Kohara et al., 2004] was induced using 100 nM of 4-hydroxytamoxifen (Sigma–Aldrich, St. Louis, MO) and passaged for 8 days (RzM6-8d) or for more than 44 days (RzM6-LC) [Nishimura et al., 2009] (Supplementary Fig. 1). Cell viability was measured using WST-8 (Dojindo, Kumamoto, Japan).

Purification and Matrix-Assisted Laser Desorption Ionization Time-of-Flight Mass Spectrometry (MALDI-TOF-MS) Analysis of p70 and TOM70 Expression Vector

p70 was identified using MALDI-TOF-MS. The p70 band was excised, alkylated using 40 mM iodoacetamide/0.1 M NH_4HCO_3, and digested using trypsin. The p70 peptides were purified using an UltiMate capillary high-performance liquid chromatography system (Dionex) and analyzed using a 4700 Proteomics Analyzer (Applied Biosystems, Foster City, CA), as described previously [Jensen et al., 1999]. An expression vector with myc and His tags was constructed for TOM70 as follows: Total RNA was isolated from HuH-7 cells (10^6) by using the ISOGEN reagent (Nippon Gene, Tokyo, Japan). Purified RNA (2 μg) was reverse transcribed using SuperScriptIII (Invitrogen, Carlsbad, CA) and oligo(dT)$_{12-18}$ primer (Invitrogen), according to the manufacturer's protocol. The coding region of TOM70 cDNA was amplified by polymerase chain reaction (PCR) with LA *Taq* polymerase (Takara Bio, Shiga, Japan) and TOM70-F2 (5′-GGATCCGCAGAGGACACTTGTCATGGC-3′), which contained a *Bam*HI restriction site (underlined), as the forward primer and TOM70-R2 (5′-GCTGGAGTGCAGTGGCTATTC-3′) as the reverse primer. The amplified TOM70 cDNA was subcloned into the pCR2.1-TOPO vector. *Bam*HI–*Eco*RI-digested TOM70 cDNA was subcloned into pcDNA6/Myc-His(+) (Invitrogen) (TOM70-pcDNA6).

Immunoprecipitation (IP) and Western Blotting (WB)

The cells were solubilized in lysis buffer (20 mM HEPES-NaOH [pH 7.5], 1 mM EDTA [pH 7.5], 1 mM dithiothreitol, 1 μM diisopropylfluorophosphate, 150 mM NaCl, and 1% TritonX-100). Samples were centrifuged at 20,400*g* for 10 min at 4°C, and the supernatants were used for IP. Protein-G sepharose 4B beads (GE Healthcare, Piscataway, NJ; 20 μl) were washed, mixed with 2-243a antibody (2 μg) in 1% BSA-phosphate-buffered saline (PBS), and placed on a rotary shaker at 4°C for 1 hr. Next, the beads were washed three times with lysis buffer and treated with the cell lysate (4°C, overnight). The IP mix was washed four times with lysis buffer and solubilized with 2× SDS sample buffer (150 mM Tris [pH 6.8], 4% SDS, 20% glycerol, 10% 2-mercaptoethanol, and 0.2% bromophenol blue). WB was performed as described previously [Nishimura et al., 2009]. Anti-myc monoclonal antibody (mAb) (9E10; Santa Cruz Biotechnology, Santa Cruz, CA), anti-HCV core mouse mAb (31-2), and anti-NS3 rabbit polyclonal antibody (R212) were used to examine the interaction between NS3 and myc-TOM70. Anti-Mcl-1 antibody (S-19; Santa Cruz Biotechnology) and anti-MAVS antibody (ab25084; ChIP grade; Abcam, Cambridge, MA) were also used. Professor Mihara (Kyusyu University) kindly provided anti-rat TOM70 polyclonal antibody (rTOM70).

Immunofluorescence Assay (IFA)

For mitochondrial staining, MitoRed (Dojindo) was added to the cell culture medium and incubated for 1 hr. The cells were fixed in 4% paraformaldehyde. The slides were then washed with PBS, permeabilized with 1% Triton X-100; and reacted with 2-243a mAb (1 μg/ml) and a polyclonal antibody against the endoplasmic reticulum (ER) (anti-PDI; 1:1,000; Stressgen Bioreagent, Kampenhout, Belgium) in 0.025% Tween-20 PBS, followed by reaction with FITC-conjugated goat anti-mouse IgG mAb (1:1,000; Cappel Products, Portland, ME) and Alexa 568-conjugated goat anti-rabbit IgG (Fab′)$_2$ fragment (Invitrogen) in 0.025% Tween-20 PBS. The slides were covered with Vector Shield (Vector Laboratories, Burlingame, CA) and observed under an Olympus Fluoview laser-scanning microscope (Olympus, Tokyo, Japan).

Evaluation of Cell Death by Assessing Fas or Tumor Necrosis Factor (TNF)-α

The cells were plated in a 96-well plate (10^4 cells/well; Becton Dickinson, Franklin Lake, NJ) and transfected with empty pcDNA6 or TOM70-pcDNA6 (40 ng/well) by using the Lipofectamine 2000 reagent (Invitrogen). After 48 hr, the cells were treated with anti-Fas

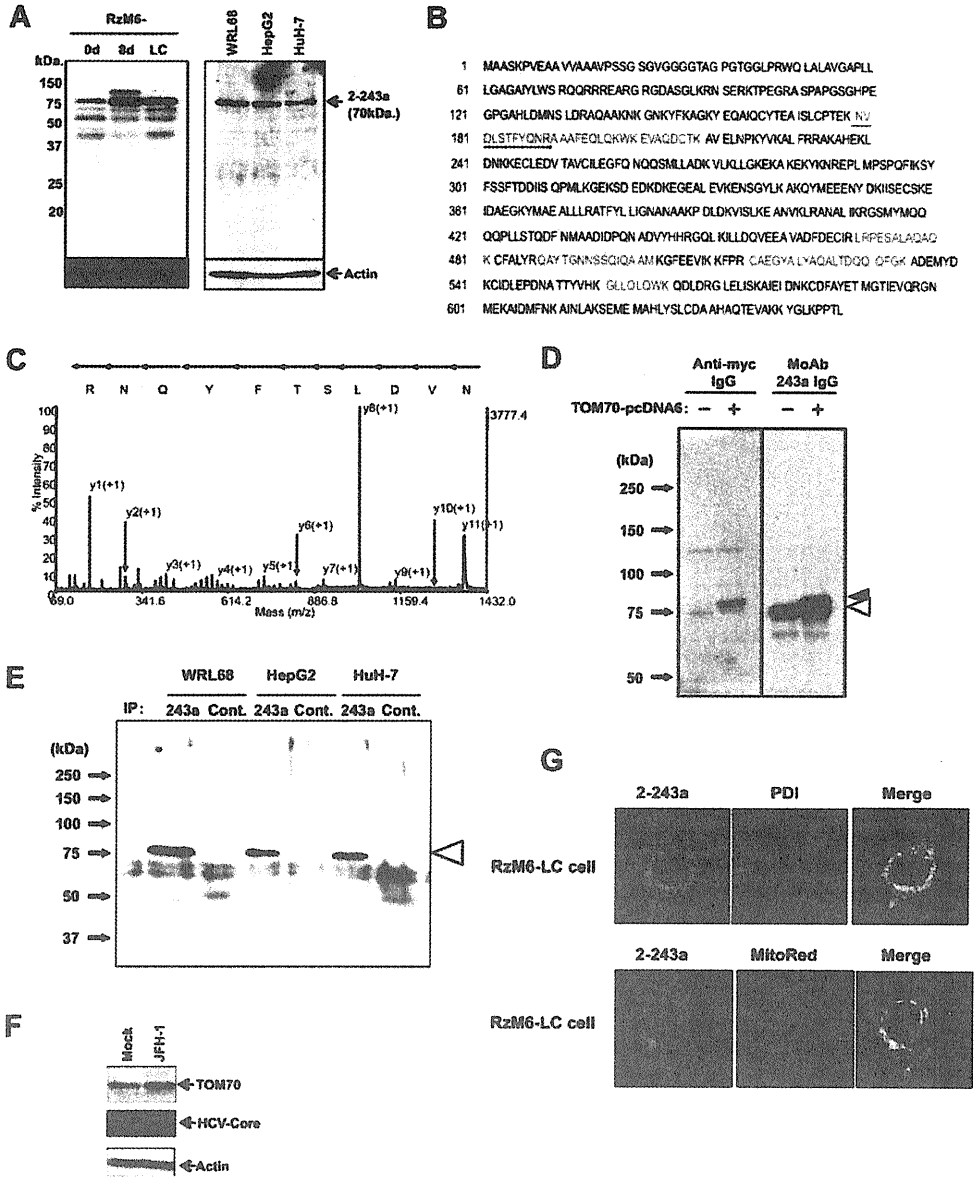

Fig. 1. TOM70 is induced by HCV and is localized in the mitochondria. A: TOM70 induction was examined by WB in RzM6-8d and RzM6-LC days (left panel), and TOM70 expression was compared in WRL68, HepG2, and HuH-7 cells (right panel). B: Identification of p70 by MALDI-TOF-MS analysis. The sequence of peptides in the amino acid sequence of TOM70 protein was determined using MALDI-TOF-MS analysis (red characters). C: MS/MS spectra of the peptide NVDLSTFYQNR (149–159). The sequence covers 14% of the amino acid sequence of TOM70. D: Identification of p70 by IP-WB. Expression of TOM70-pcDNA6 in HuH-7. Cell lysates were examined using WB with mAb 2-243a or the anti-myc antibody. myc-TOM70-pcDNA6 expression was recognized by both mAb 2-243a and the anti-myc antibody (black triangle). The expression of cellular TOM70 (empty triangle) was recognized only by mAb 2-243a. E: Cell lysates were immunoprecipitated with anti-rat TOM70 antibody and analyzed using WB with mAb 2-243a. The empty triangle indicates TOM70. The molecular weight markers are shown on the left. F: Expression of TOM70 and the core protein in mock- and HCV JFH-1-infected HuH-7 cells. G: Localization of TOM70 in RzM6-LC cells. The cells were stained with mAb 2-243a and polyclonal antibody against PDI or MitoRed. The magnification is 800×.

antibody (CH-11; 0–20 ng/ml; Beckman Coulter, Murmasaka) or recombinant human TNF-α (0–100 ng/ml; PeproTech, Rocky Hill, NJ), followed by addition of cycloheximide (CHX; 10 μg/ml). After treatment for 24 hr, apoptotic cell death was evaluated by determining cell viability with the WST-8 reagent. Next, the terminal deoxynucleotidyl transferase dUTP nick-end labeling (TUNEL) assay was performed using the TMR red in situ cell death detection kit (Roche, Basel, Switzerland).

Generation of Small Interfering Ribonucleic Acid (siRNA) for TOM70

siRNAs for two regions of TOM70, namely, TOM70-d1-siRNA (primer set: TOM70-dicer1-F and TOM70-dicer1-R) and TOM70-d2-siRNA (primer set: TOM70-dicer2-F and TOM70-dicer2-R) were generated.

Gene-specific dsDNA for TOM70 was constructed by PCR using TOM70-pcDNA6 as the template. TOM70-dicer1-F (5′-GCGTAATACGACTCACTATAGGGAGA-TGTTTGGCCTTTAAGTATCC-3′) was used as the forward primer, and TOM70-dicer1-R (5′-GCGTAA-TACGACTCACTATAGGGAGATGATATCATCCGTGA-AAGAAC-3′) was used as the reverse primer; both primers contained a T7 promoter sequence (underlined). PCR performed using these primers yielded a 434-bp product. PCR with the forward primer TOM70-dicer2-F (5′-GCGTAATACGACTCACTATAGGGAGAATGTTTG-CATTGTACCGCC-3′) and the reverse primer TOM70-dicer2-R2 (5′-GCGTAATACGACTCACTATAGGGAGA-TTTGCAACTTCTGTCTGGGC-3′), both of which contained a T7 promoter sequence (underlined), yielded a 474-bp product. Luciferase was amplified from pGL3-Basic (Takara Bio) with Luci-dicer2-F (5′-GCGTAA-TACGACTCACTATAGGGAGACGGTTTTGGAATGTT-TACTAC-3′) as the forward primer and Luci-dicer2-R (5′-GCGTAATACGACTCACTATAGGGAGAGCTGAT-GTAGTCTCAGTGAGC-3′), as the reverse primer, yielding a 309-bp product; both primers contained a T7 promoter sequence (underlined). LA *Taq* polymerase was used for the PCR. All PCR products were analyzed by agarose electrophoresis before purification with the Wizard SV Gel and PCR Clean-Up System (Promega, Madison, WI).

In vitro transcription was performed with the Dicer siRNA generation kit (Genlantis, San Diego, CA), according to the manufacturer's instructions. Briefly, in vitro transcription reactions were performed in a 20-μl volume with 1 μg PCR product as the template; the reaction mixture was incubated at 37°C for 4 hr, followed by purification with the reagents provided in the Dicer siRNA generation kit. The dsDNA (20 μl) obtained was finally in a 100-μl volume after incubation at 37°C for 27 hr. The siRNAs obtained were purified and quantified according to the manufacturer's instructions.

Next, the cells were plated in 24- or 96-well plates (BD Bioscience, Sparks, MD) at a density of 5×10^4 or 10^4 cells/well, respectively, and left overnight for adherence. The siRNAs (14 nM) generated were transfected to cells by using Lipofectamine RNAiMAX (Invitrogen) and Opti-MEM (Invitrogen). The cells were characterized 48 hr after transfection.

Caspase Assay

The activities of caspase-3/7, caspase-8, and caspase-9 were measured on the basis of the cleavage of a proluminescent substrate containing the DEVD sequence, by using the commercially available Caspase-Glo 9 Assay, Caspase-Glo 8 Assay, and Caspase-Glo 3/7 Assay kits (Promega) and a luminometer (Aloka, Tokyo, Japan). Caspase activity was quantified according to the manufacturer's instructions.

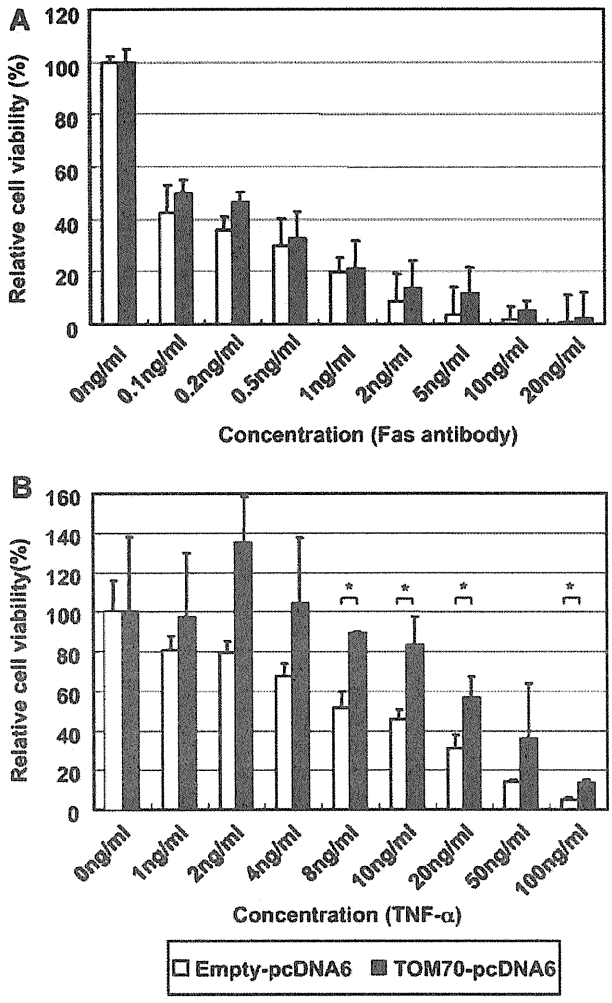

Fig. 2. TOM70 overexpression induced TNF-α-mediated apoptotic resistance. TOM70 overexpression affected TNF-α-mediated apoptosis but not Fas-mediated apoptosis. Cells were transfected with empty pcDNA6 (white bar) or TOM70-pcDNA6 (black bar). After 48 hr, they were treated with (A) Fas antibody (0–20 ng/ml) or (B) TNF-α (0–100 ng/ml). After 24 hr, cell viability was measured using WST-8. A,B: The data represent the average of the values obtained from triplicate experiments, and the vertical bars indicate the SD. $^*P < 0.05$ (two-tailed Student's *t*-test).

Statistical Analysis

Data were analyzed for statistical significance by using the Student's *t*-test. *P*-values lower than 0.05 were considered statistically significant.

RESULTS

Identification of the p70 Molecule and Induction by HCV

mAbs against RzM6-LC cells were screened, and the clone 2-243a, which recognizes p70, was obtained

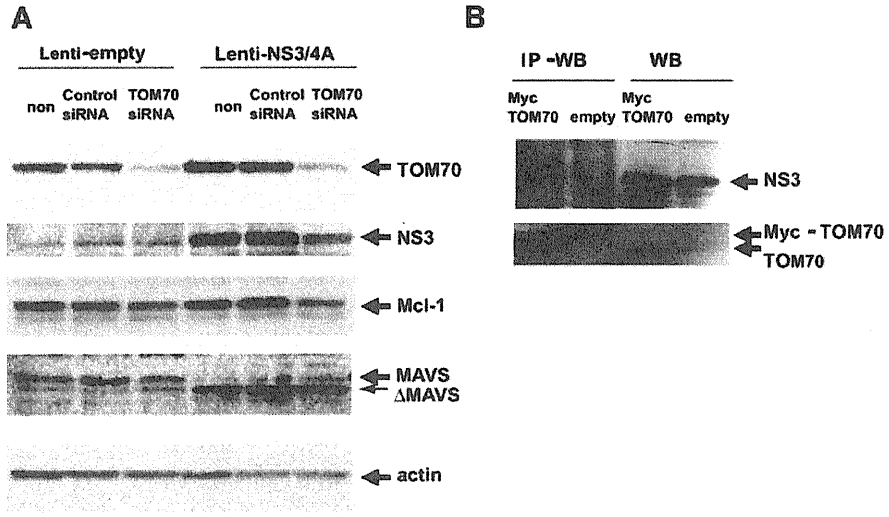

Fig. 3. Interaction between TOM70 and NS3 protein. **A**: The effect of TOM70 siRNA in cells transfected with empty or NS3/4A-containing lentivirus vectors was examined by WB with mAb 2-243a for TOM70; anti-NS3 rabbit polyclonal antibody; anti-Mcl-1 rabbit polyclonal antibody; anti-MAVS rabbit polyclonal antibody; and anti-actin antibody. **B**: The interaction between TOM70 and NS3 was assessed using IP-WB. NS3-expressing HepG2 cells were transfected with pcDNA6-TOM70 (mycTOM70) or pcDNA6 alone (empty) and immunoprecipitated with the anti-myc antibody (9E10). NS3 was detected using polyclonal rabbit anti-NS3 antibody (upper image), and TOM70 was detected using mAb 2-243a (lower image).

(Fig. 1A). p70 was induced to a greater extent by HCV expression after 8 days (RzM6-8d) or more than 44 days (RzM6-LC) than before HCV expression (RzM6-0d). The p70 expression level did not differ among the human hepatic cell lines (WRL68, HepG2, and HuH-7) (Fig. 1A, right panel). p70 was characterized (Fig. 1B–E): The sequence of peptides determined using MALDI-TOF-MS (Fig. 1B) and the MS/MS spectra of the p70 peptide sequence NVDLSTFYQNR (Fig. 1C) are provided. TOM70-pcDNA6 expression in HuH-7 cells was detected by WB with mAb 2-243a (Fig. 1D). Cell lysates were immunoprecipitated with anti-rat TOM70 antibody and detected by WB using mAb 2-243a (Fig. 1E). These results indicate that mAb 2-243a recognizes TOM70. Next, the effect of HCV infection on TOM70 expression was examined (Fig. 1F), and infection with the HCV JFH-1 strain [Wakita et al., 2005] induced TOM70 expression in HuH-7 cells (Fig. 1F). TOM70 localization was characterized using an indirect fluorescence assay (IFA) with 2-243a; anti-PDI, an ER marker; or MitoRed, which is a selective mitochondrial marker (Fig. 1G). TOM70 was associated with the mitochondria in all cells and was a part (~40%) of the ER, indicating that the TOM70 expressions in the mitochondria were higher than those in the ER.

TOM70 Inhibits TNF-α-Mediated Apoptotic Cell Death

The results of previous studies indicate the significant role of mitochondria in the apoptotic response [Hatano, 2007]. TOM70 interacts with Mcl-1 and facilitates mitochondrial targeting by the latter [Chou et al., 2006]. Mcl-1 silencing enhances TNF-related apoptosis-inducing ligand (TRAIL)-mediated cell death [Wirth et al., 2005; Han et al., 2006]. Therefore, the role of TOM70 in the apoptotic response was examined in this study. HepG2 cells were transfected with TOM70-pcDNA6 (Fig. 1D) or empty pcDNA6 (control), and their sensitivity to anti-Fas antibody (Fig. 2A) and TNF-α-mediated apoptotic cell death (Fig. 2B) was examined. When treated with 8 ng/ml of TNF-α, the TOM70-pcDNA6-transfected cells were significantly more viable than those transfected with empty pcDNA6 (Fig. 2B). In contrast, no significant differences were found between the viability of TOM70-pcDNA6 transfected cells and control cells treated with anti-Fas antibody (Fig. 2A). Thus, TNF-α-induced apoptosis was inhibited by TOM70 overexpression.

Interaction of TOM70 With HCV-NS3 and Other Host Factors

To determine the mechanism by which HCV induces TOM70, the TOM70 level in HCV NS3/4A-expressing HepG2 cells was determined (Fig. 3A). The TOM70 level was higher in the NS3/4A-expressing cells than in the control cells. Interestingly, the level of NS3/4A protein as well as Mcl-1 was reduced when TOM70 was silenced. The MAVS protein is cleaved by NS3/4A, as reported previously [Li et al., 2005], and the level of this protein was not influenced by the silencing of TOM70. IP-WB was performed to examine the possible interaction between TOM70 and NS3/4A (Fig. 3B). The pcDNA6-TOM70-myc plasmid was transfected into lenti-NS3/4A vector-transduced HepG2 cells; IP was performed using the anti-myc antibody, and the reaction was detected using the anti-NS3 antibody. The NS3 protein was

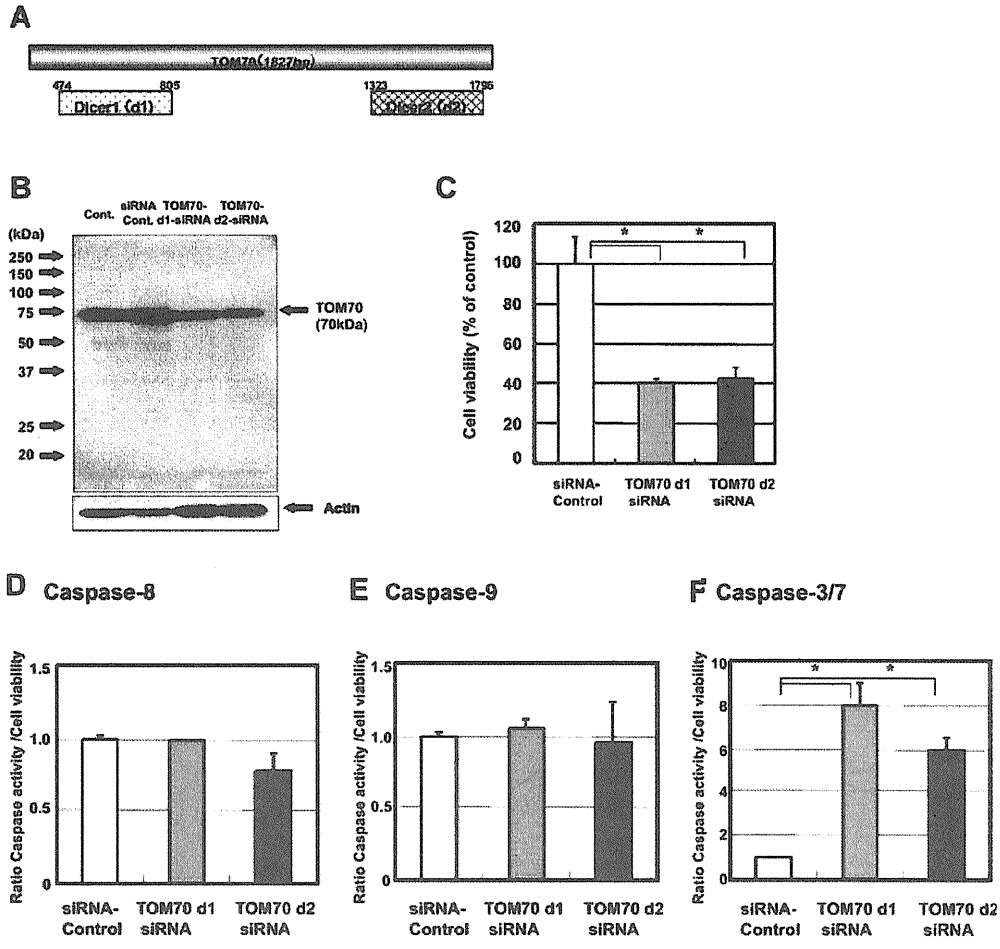

Fig. 4. Silencing of TOM70 induced apoptotic cell death and caspase-3/7 activity. A: The positions of TOM70-d1-siRNA and TOM70-d2-siRNA are indicated in the figure. B: siRNA-mediated silencing of TOM70 was detected by WB (Cont: no siRNA, siRNA Cont: siRNA control (Luci2-siRNA), TOM70-d1-siRNA, TOM70-d2-siRNA). C: TOM70 knockdown-induced cell death was calculated by measuring viability (%) with the WST-8 cell counting kit. The cell viability after 48 hr was scored in HepG2 cells transfected with the siRNA control Luci2-siRNA (□), TOM70-d1-siRNA (■), and TOM70-d2-siRNA (■). The activities of caspase-8 (D), caspase-9 (E), and caspase-3/7 (F) were measured using commercially available assays and a luminometer. The caspase activity was scored after 48 hr in TOM70-knockdown HepG2 cells transfected with control siRNA (□), TOM70-d1-siRNA (■), and TOM70-d2-siRNA (■). C–F: The data represent the average of the values obtained from triplicate experiments, and the vertical bars indicate the SD. $^*P < 0.05$ (two-tailed Student's t-test).

specifically precipitated by myc-tagged TOM70. The NS4A protein was not detected in this assay (data not shown). Therefore, the NS3 protein directly interacts with TOM70.

TOM70 Knockdown by RNAi Induces Apoptosis

The effect of TOM70 on the apoptotic response was examined because TOM70 silencing decreased the level of Mcl-1. First, two siRNAs for TOM70 (TOM70-d1-siRNA and TOM70-d2-siRNA) were designed in order to prevent the off-target effect (Fig. 4A). siRNA for luciferase (Luci-d2-siRNA) was used as a control (Fig. 4B). HepG2 cells were transfected with TOM70-d1-siRNA or TOM70-d2-siRNA, and the downregulation of TOM70 expression was confirmed by WB (Fig. 4B). Furthermore, decreased cell viability was observed (Fig. 4C) after 48 hr. Treatment with TOM70-d1-siRNA or TOM70-d2-siRNA significantly decreased the cell viability of HuH-7 cells too (data not shown). These results indicate that TOM70 silencing with siRNA may induce apoptosis.

The activities of caspase-3/7, caspase-8, and caspase-9 in HepG2 cells were examined after TOM70 silencing (Fig. 4D–F). The activities of caspase-8 and caspase-9 in cells transfected with TOM70 siRNA were not significantly different from those in the cells treated with control siRNA (Fig. 4D,E). In contrast, the caspase-3/7 activity in the TOM70-siRNA transfected cells was significantly greater than that in the cells treated with

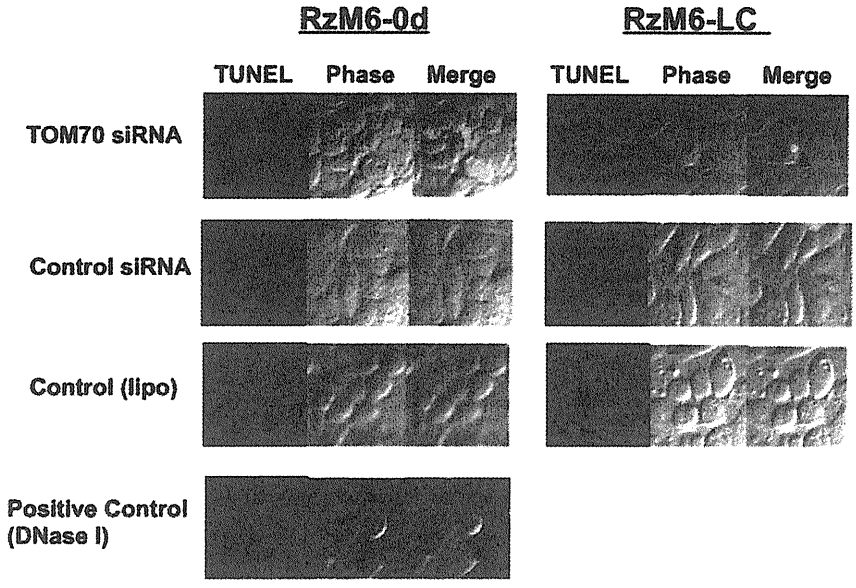

Fig. 5. TUNEL assay in RzM6-0d and RzM6-LC cells transfected with TOM70 siRNA, control siRNA, and control (Lipofectamine). The positive control is RzM6-0d cells treated with DNase I. The magnification is 400×.

control siRNA (Fig. 4F). These results indicate that the siRNA-mediated silencing of TOM70 expression induces apoptosis through caspase-3/7.

TOM70 Silencing-Induced Apoptosis Is Impaired by HCV

Next, the effect of TOM70 silencing-induced apoptosis was examined in RzM6-0d and RzM6-LC cells in order to determine the effect of HCV expression (Fig. 5). The apoptotic response was examined using the TUNEL assay wherein DNA strand breaks are detected and the apoptotic response is thereby detected [Gavrieli et al., 1992]. The DNA strand breaks, which were stained red, were observed using confocal microscopy. Treatment with TOM70 siRNA produced significant DNA strand breaks in the RzM6-0d cells. However, the apoptotic signal was suppressed in the RzM6-LC cells. This indicates the possibility that HCV can impair the apoptotic response induced by TOM70 siRNA.

Silencing of TOM70 Decreases Cell Viability, Whereas HCV-NS3 Restores Cell Viability

The RzM6-0d and RzM6-LC cells were treated with TOM70 siRNA and control siRNA, and the cell viability was measured using the WST-8 assay [Isobe et al., 1999] (Fig. 6A). The viability of the RzM6-LC cells was significantly higher than that of the RzM6-0d cells after treatment with TOM70 siRNA, and this difference increased in a dose-dependent manner. This indicates that the expression of HCV genes may impair the TOM70 siRNA-induced apoptotic response. The responsible HCV protein was identified using the lentivirus vector (Fig. 6B), and TOM70 siRNA-induced cell death was found to be impaired in HCV-NS3/4A-expressing cells.

DISCUSSION

The results of the present study suggest that HCV interacts with TOM70 through the NS3 protein, which indicates the possibility that TOM70 regulates the intracellular localization of HCV NS3; a previous study has reported the mitochondrion to be one of the regions where HCV NS3 is located [Sillanpaa et al., 2008]. The results of a previous study indicate that TOM70 also interacts with the Mcl-1 protein [Chou et al., 2006]. TOM70 silencing decreased the levels of the NS3 and Mcl-1 proteins; therefore, interaction with TOM70 may increase the stability of NS3 and Mcl-1. Recently, it was reported that Mcl-1 is stabilized by the deubiquitinase USP9X and that it can promote tumor cell survival [Schwickart et al., 2010]. Furthermore, Mcl-1 interacts with the HCV core protein through Bcl-2 homology domain 3 (BH3) [Mohd-Ismail et al., 2009], and Mcl-1 overexpression suppresses core-induced apoptosis. Therefore, further studies are required to clarify the relationship between TOM70, Mcl-1, and other host factors in HCV infection. This information may provide novel insights into the mechanism underlying the induction of apoptotic resistance and tumorigenicity in hepatocytes during chronic HCV infection.

The results of this study indicate the regulatory role of TOM70 in apoptosis. TOM70 overexpression was found to suppress the TNF-α-mediated but not the Fas-mediated apoptotic response. TOM70 knockdown

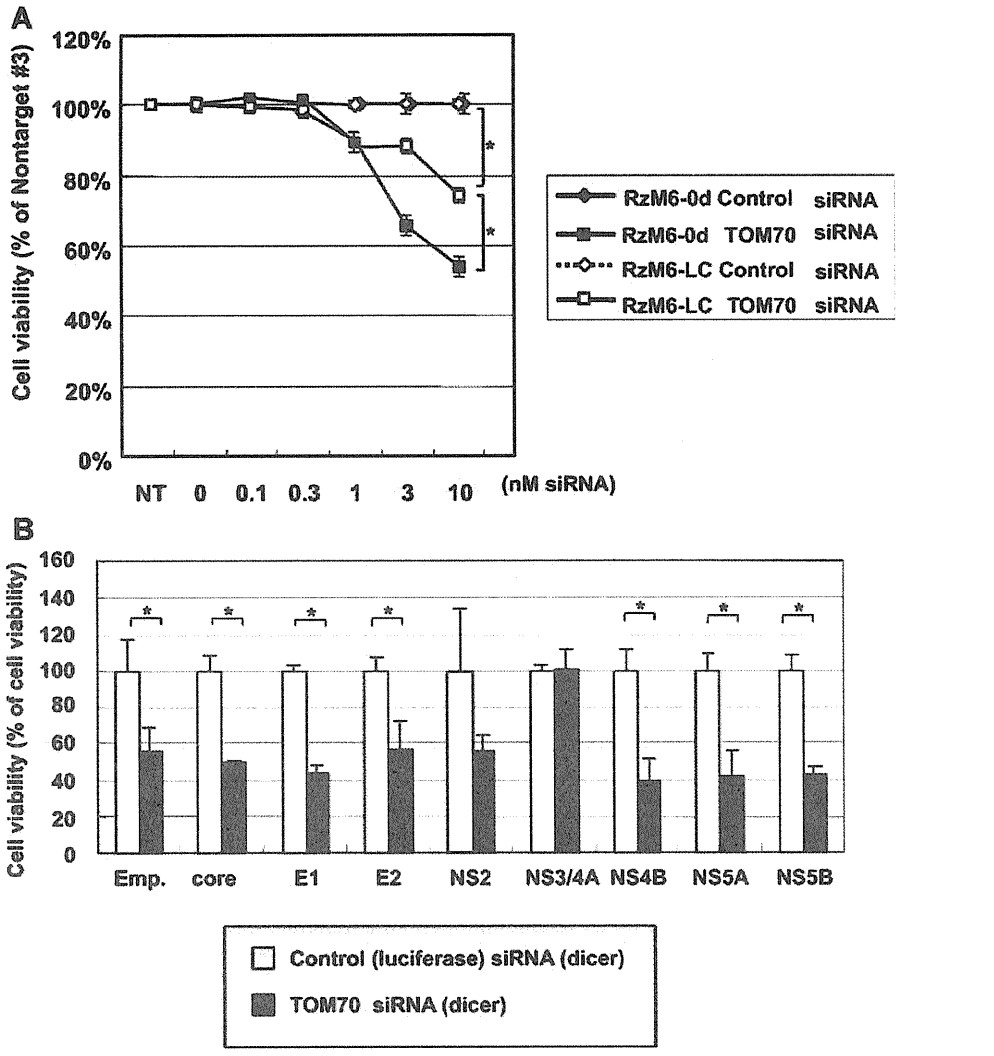

Fig. 6. A: Cell viability of RzM6-0d or RzM6-LC cells after treatment with TOM70 siRNA. The viability is given as the ratio (%) of test to control siRNA treatment. B: The viability of HepG2 cells transduced with lentivirus vectors expressing the HCV core, E1, E2, NS2, NS3/4A, NS4B, NS5A, and NS5B proteins after treatment with TOM70 siRNA was measured by the WST assay, and the viability is given as the ratio (%) of the test to the control siRNA treatment. The data represents the average of the values obtained from triplicate experiments, and the vertical bars indicate SD. $^*P < 0.05$ (two-tailed Student's t-test).

increased caspase-3/7 activity, but the activities of caspase-8 and caspase-9 were not significantly affected. This indicates the possibility that TOM70 regulates the TNF receptor-mediated apoptotic pathway. Several reports have indicated that TNF-α-mediated apoptosis is inhibited by HCV proteins. Saito et al. [2006] reported that the HCV core protein inhibited the TNF-α-mediated signaling pathway through the sustained expression of a cellular- FADD-like interleukin-1β-converting enzyme (FLICE) like inhibitory protein (c-FLIP; caspase-8 inhibitor). Majumder et al. [2002] reported that TNF-α-mediated hepatic apoptosis was impaired by the HCV-NS5A protein. The results of the present study revealed an alternative pathway by which HCV can acquire TNF-α-induced apoptotic resistance through TOM70 augmentation. Recently, it has been reported that TOM70 interacts with MAVS, TNFRSF1A-associated via death domain (TRADD), TNF receptor-associated factor 6 (TRAF6), stimulator of interferon genes (STING), and interferon regulatory factor (IRF)-3, and that augmentation of TOM70 activates retinoic acid-inducible gene (RIG)-I signaling [Liu et al., 2010]. The results of recent studies indicate that IRF-3 can activate Bax expression and apoptosis [Chattopadhyay et al., 2004]. Future studies on the modification of the regulatory pathway of TOM70 by HCV may provide further insights on the mechanism underlying persistent HCV infection.

ACKNOWLEDGMENTS

The authors thank Dr. H. Fukuda and Dr. S. Ohmi for their technical support with regard to MALDI-TOF-MS analysis, Dr. F. Yasui and Dr. T. Munakata for their critical comments, Dr. Satoh for his technical support, and Prof. S. Harada for his support.

REFERENCES

Chattopadhyay S, Marques JT, Yamashita M, Peters KL, Smith K, Desai A, Williams BR, Sen GC. 2004. Viral apoptosis is induced by IRF-3-mediated activation of Bax. EMBO J 29:1762–1773.

Chou CH, Lee RS, Yang-Yen HF. 2006. An internal EELD domain facilitates mitochondrial targeting of Mcl-1 via a Tom70-dependent pathway. Mol Biol Cell 17:3952–3963.

Deng L, Adachi T, Kitayama K, Bungyoku Y, Kitazawa S, Ishido S, Shoji I, Hotta H. 2008. Hepatitis C virus infection induces apoptosis through a Bax-triggered, mitochondrion-mediated, caspase 3-dependent pathway. J Virol 82:10375–10385.

Gavrieli Y, Sherman Y, Ben-Sasson SA. 1992. Identification of programmed cell death in situ via specific labeling of nuclear DNA fragmentation. J Cell Biol 119:493–501.

Han J, Goldstein LA, Gastman BR, Rabinowich H. 2006. Interrelated roles for Mcl-1 and BIM in regulation of TRAIL-mediated mitochondrial apoptosis. J Biol Chem 281:10153–10163.

Hatano E. 2007. Tumor necrosis factor signaling in hepatocyte apoptosis. J Gastroenterol Hepatol 22:S43–S44.

Hoogenraad NJ, Ward LA, Ryan MT. 2002. Import and assembly of proteins into mitochondria of mammalian cells. Biochim Biophys Acta 1592:97–105.

Isobe I, Michikawa M, Yanagisawa K. 1999. Enhancement of MTT, a tetrazolium salt, exocytosis by amyloid beta-protein and chloroquine in cultured rat astrocytes. Neurosci Lett 266:129–132.

Jensen ON, Wilm M, Shevchenko A, Mann M. 1999. Sample preparation methods for mass spectrometric peptide mapping directly from 2-DE gels. Methods Mol Biol 112:513–530.

Lei Y, Moore CB, Liesman RM, O'Connor BP, Bergstralh DT, Chen ZJ, Pickles RJ, Ting JP. 2009. MAVS-mediated apoptosis and its inhibition by viral proteins. PLoS One 4:e5466.

Li XD, Sun L, Seth RB, Pineda G, Chen ZJ. 2005. Hepatitis C virus protease NS3/4A cleaves mitochondrial antiviral signaling protein off the mitochondria to evade innate immunity. Proc Natl Acad Sci USA 102:17717–17722.

Liu XY, Wei B, Shi HX, Shan YF, Wang C. 2010. Tom70 mediates activation of interferon regulatory factor 3 on mitochondria. Cell Res 20:994–1011.

Majumder M, Ghosh AK, Steele R, Zhou XY, Phillips NJ, Ray R, Ray RB. 2002. Hepatitis C virus NS5A protein impairs TNF-mediated hepatic apoptosis, but not by an anti-FAS antibody, in transgenic mice. Virology 294:94–105.

Mihara K, Omura T. 1996. Cytoplasmic chaperones in precursor targeting to mitochondria: The role of MSF and hsp 70. Trends Cell Biol 6:104–108.

Mohd-Ismail NK, Deng L, Sukumaran SK, Yu VC, Hotta H, Tan YJ. 2009. The hepatitis C virus core protein contains a BH3 domain that regulates apoptosis through specific interaction with human Mcl-1. J Virol 83:9993–10006.

Neupert W. 1997. Protein import into mitochondria. Annu Rev Biochem 66:863–917.

Nishimura T, Kohara M, Izumi K, Kasama Y, Hirata Y, Huang Y, Shuda M, Mukaidani C, Takano T, Tokunaga Y, Nuriya H, Satoh M, Saito M, Kai C, Tsukiyama-Kohara K. 2009. Hepatitis C virus impairs p53 via persistent overexpression of 3beta-hydroxysterol Delta24-reductase. J Biol Chem 284:36442–36452.

Nomura-Takigawa Y, Nagano-Fujii M, Deng L, Kitazawa S, Ishido S, Sada K, Hotta H. 2006. Non-structural protein 4A of Hepatitis C virus accumulates on mitochondria and renders the cells prone to undergoing mitochondria-mediated apoptosis. J Gen Virol 87: 1935–1945.

Pfanner N, Geissler A. 2001. Versatility of the mitochondrial protein import machinery. Nat Rev Mol Cell Biol 2:339–349.

Pfanner N, Meijer M. 1997. The Tom and Tim machine. Curr Biol 7:R100–R103.

Saito K, Meyer K, Warner R, Basu A, Ray RB, Ray R. 2006. Hepatitis C virus core protein inhibits tumor necrosis factor alpha-mediated apoptosis by a protective effect involving cellular FLICE inhibitory protein. J Virol 80:4372–4379.

Saitou K, Mizumoto K, Nishimura T, Kai C, Tsukiyama-Kohara K. 2009. Hepatitis C virus-core protein facilitates the degradation of Ku70 and reduces DNA-PK activity in hepatocytes. Virus Res 144: 266–271.

Schatz G. 1996. The protein import system of mitochondria. J Biol Chem 271:31763–31766.

Schwickart M, Huang X, Lill JR, Liu J, Ferrando R, French DM, Maecker H, O'Rourke K, Bazan F, Eastham-Anderson J, Yue P, Dornan D, Huang DC, Dixit VM. 2010. Deubiquitinase USP9X stabilizes MCL1 and promotes tumour cell survival. Nature 463: 103–107.

Seeff LB. 2002. Natural history of chronic hepatitis C. Hepatology 36:S35–S46.

Sillanpaa M, Kaukinen P, Melen K, Julkunen I. 2008. Hepatitis C virus proteins interfere with the activation of chemokine gene promoters and downregulate chemokine gene expression. J Gen Virol 89:432–443.

Stojanovski D, Johnston AJ, Streimann I, Hoogenraad NJ, Ryan MT. 2003. Import of nuclear-encoded proteins into mitochondria. Exp Physiol 88:57–64.

Truscott KN, Pfanner N, Voos W. 2001. Transport of proteins into mitochondria. Rev Physiol Biochem Pharmacol 143:81–136.

Tsukiyama-Kohara K, Tone S, Maruyama I, Inoue K, Katsume A, Nuriya H, Ohmori H, Ohkawa J, Taira K, Hoshikawa Y, Shibasaki F, Reth M, Minatogawa Y, Kohara M. 2004. Activation of the CKI-CDK-Rb-E2F pathway in full genome hepatitis C virus-expressing cells. J Biol Chem 279:14531–14541.

Wakita T, Pietschmann T, Kato T, Date T, Miyamoto M, Zhao Z, Murthy K, Habermann A, Krausslich HG, Mizokami M, Bartenschlager R, Liang TJ. 2005. Production of infectious hepatitis C virus in tissue culture from a cloned viral genome. Nat Med 11: 791–796.

Wirth T, Kuhnel F, Fleischmann-Mundt B, Woller N, Djojosubroto M, Rudolph KL, Manns M, Zender L, Kubicka S. 2005. Telomerase-dependent virotherapy overcomes resistance of hepatocellular carcinomas against chemotherapy and tumor necrosis factor-related apoptosis-inducing ligand by elimination of Mcl-1. Cancer Res 65:7393–7402.

Exp. Anim. 60(2), 93–100, 2011

—Review—
Review Series: Frontiers of Model Animals for Human Diseases

An Experimental Mouse Model for Hepatitis C Virus

Kiminori KIMURA[1, 2] and Michinori KOHARA[1]

[1]*Department of Microbiology and Cell Biology, Tokyo Metropolitan Institute of Medical Science, Tokyo 156-8506 and* [2]*Division of Hepatology, Tokyo Metropolitan Cancer and Infectious Diseases Center, Komagome Hospital, Tokyo 113-8677, Japan*

Abstract: Chronic hepatitis C virus (HCV) infection affects approximately 170 million people and is a major global health problem because infected individuals can develop liver cirrhosis and hepatocellular carcinoma. Despite significant improvements in antiviral drugs, only around 50% of treated patients with genotype 1 and 4 demonstrate HCV clearance. Unfortunately, an anti-HCV vaccine is still not available. To progress treatment of HCV, it is necessary to understand the mechanism(s) by which HCV infects hepatocytes, and how the host immune response prevents the spread of the virus. Because HCV infects only humans and chimpanzees, it is difficult to evaluate immune response mechanisms, and the effects of chemicals and new technologies on these response mechanisms. These difficulties underline the importance of establishing a small HCV-infected animal model. This review focuses on the progress made in recent years towards the development of an experimental mouse model for HCV.
Key words: apoptosis, B cell lymphoma, HCV, immune response, transgenic mice

Introduction

Hepatitis C virus (HCV) is a non-cytopathic, hepatotropic member of the *Flaviviridae* family, causing acute and chronic necroinflammatory liver diseases [25]. Chronic HCV infection has caused an epidemic with approximately 170 million people infected worldwide and three to four million people newly infected each year [25, 35]. Natural history studies show that 5–20% of patients develop cirrhosis after about 20 years of infection [1, 42, 49]. An increasing number of patients with cirrhosis will develop hepatocellular carcinoma. End-stage liver disease due to chronic HCV infection is the leading cause of liver transplantation in the western world [36]. Furthermore, co-infection with HCV and human immunodeficiency virus (HIV) results in more serious liver cirrhosis than HCV infection alone and the mortality of HIV-infected HCV patients is a serious problem in the USA [44. 55].

The HCV genome is a 9.6-kb, uncapped, linear, single-strand RNA molecule with positive polarity that serves as a template for both translation and replication. Translation of the plus-strand RNA initiates at an internal ribosomal entry site, resulting in the production of a single polyprotein precursor that is processed into structural (C, E1, E2, p7) and non-structural (NS2, NS3, NS4A, NS4B, NS5A, and NS5B) protein subunits by host and viral proteases [8, 9, 37, 46]. Because of the lack of a proofreading func-

(Received 20 December 2010 / Accepted 29 January 2010)
Address corresponding: M. Kohara, Department of Microbiology and Cell Biology, Tokyo Metropolitan Institute of Medical Science, 2–1–6 Kamikitazawa, Setagaya-ku, Tokyo 156-8506, Japan